leti
cea tech

ANNUAL
RESEARCH REPORT
2015

OPTICS AND PHOTONICS

Leti, technology research institute

TECHNOLOGY RESEARCH INSTITUTE

LETI AT A GLANCE

Founded in **1967**

Based in **France** (Grenoble)
with offices in **USA** (Silicon Valley)
and **Japan** (Tokyo)

350
industrial partners

1,900
researchers

Committed to innovation, Leti's teams create **differentiating solutions in miniaturization and energy-efficient technologies** for its industrial partners.

Leti is a technology research institute at CEA Tech and a recognized global leader focused on miniaturization technologies enabling energy-efficient and secure IoT. Leti delivers solid expertise throughout the entire IoT chain, from sensors to data processing and computing solutions. Leti pioneered FDSOI low power platform for IoT, M&NEMS technology for low cost multisensors solutions, CoolCube™ integration for highly connected and cost effective devices.

Leti's mission is to pioneer new technologies, enabling innovative solutions to ensure Leti's industrial partners competitiveness while creating a better future. It tackles most current global issues such as the future of industry, clean and safe energies, health and wellness, sustainable transport, information and communication technologies, space exploration and safety & security.

For 50 years, the institute has built long-term relationships with its partners: global industrial companies, SMEs and startups. It tailors innovative and differentiating solutions that strengthen their competitiveness and contribute to creating new jobs. Leti and its partners work together through bilateral projects, joint laboratories and collaborative research programs. Leti actively contributes to the creation of startups through its startup program.

Leti has signed partnerships with major research technology organizations and academic institutions. It is a member of the Carnot Institutes network*.

**Carnot Institutes network: French network of 34 institutes serving innovation in industry.*

2,670
patents in portfolio

60
startups created

€315
million budget

700
publications each year

ISO 9001
certified since 2000

OPTICS AND PHOTONICS

Within CEA Tech and Leti, **Optics and Photonics** activities are focused principally on big industrial markets for photonics: all-wavelength imaging (visible, infrared, THz), information displays, solid state lighting, optical data communications, optical environmental sensors.

The R&D projects involved with industrial and academic partners. The industrial partners of the Optics and Photonics Division range from SMEs to large international companies. The projects merge fundamental aspects with advanced technological and industrial developments; nanosciences are connected with material sciences, optics, electronics and micro- & nano-fabrication.

Picture on the cover page: MICROOLED 5.4 Mega pixels, 0.61'' (1.55cm) diagonal OLED microdisplay. OLED microdisplays technology has been developed in collaboration with the Optics and Photonics division of Leti, since 2007. MICROOLED is a privately held company, located in Grenoble, which makes high performance microdisplays for Near-Eye applications.

Contents

Edito

Ludovic POUPINET

Head of Optics and Photonics Division

Leti's Optics and Photonics Division (DOPT) aims to foster employment in France and Europe by developing innovative photonic components. We see miniaturization and integration as the main driving factors to reach this target. We help our industrial partners to decrease the cost, to improve the performances and to diversify the functionalities of their products.

DOPT is focused on various topics such as visible, infrared and THz imaging sensors as well as integrated photonic components, optical gas sensors and light emitting arrays both for displays and smart lighting. In each area, DOPT, with its 300 staff members, concentrates long-term expertise, up-to-date clean rooms and equipment and dedicated characterization benches. 90% of our funding is obtained through one-to-one or collaborative projects, both with academic and industrial partners. The high quality of our partners is one of our strengths.

To stay at the leading edge of applied photonic research requires a deep understanding of product-and-application requirements in terms of performance, cost and functions, as well as an ability to introduce new concepts in our process flows. In this report you will see how DOPT is achieving this in its different research areas. How can we grow GaN on silicon and integrate several functions to prepare integrated low-cost smart lighting? How will nanostructured materials increase the efficiency of imaging arrays and gas sensors? How will material research open the way toward high performance infrared image sensors for space applications or allow the integration of Germanium based lasers directly on Silicon? How will the adaptation of existing technologies allow us to extend the range of applications for instance in THz imaging?

I hope that reading this report will make you want to know more about us, meet us during conferences, professional forums or Leti events, join us as researcher, PhD or a post-doctoral fellow and, of course, build fruitful collaborations on exciting research topics that tackle the microscopic behavior of photons using state-of-the-art. industry-compatible facilities.

Happy reading!

Key facts and figures

200 permanent researchers
30 PhD students and Post-docs
45 CEA experts: with 2 directors of research and 2 international experts

125 publications in 2015 including 40 papers in peer-reviewed journals

65 patents filed in 2015
450 patents in portfolio with about **20%** under license

Dedicated clean-rooms for III-V and II-VI materials on versatile substrate geometries up to 150 mm
Access to Leti clean-rooms in 200 and 300 mm-processes through numerous photonic processes and technology modules

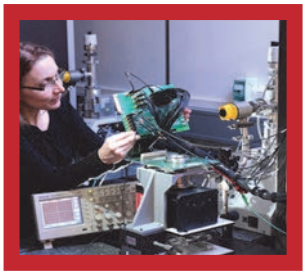

Optics and opto-electronics characterization facilities

Advanced means of modeling and simulation

Scientific Activity

Awards

Jean Marc FEDELI received in 2015 (with Alcatel Lucent Bell lab, IEF, III-V lab and Foton) the **"best paper award"** at the European Conference on Optical Communication (ECOC) with a Silicon Photonics component for optical networks.

François TEMPLIER received the **"global innovation award"** at the TechConnect World 2015 for a new GaN microdisplay with very high brightness.

Conference and workshops organization

Jean Marc FEDELI at the conference SPIE MicroTechnologies: Symposium of « Integrated Photonics: Materials, Devices, and Applications » (Barcelona, Spain)

Tony MAINDRON at the RAFALD workshop on Atomic Layer Deposition (ALD) techniques (Grenoble, France)

Sylvie MENEZO at two Silicon Photonics conferences: Optical Fiber Communication (OFC-Los Angeles, USA) and the European Conference on Optical Communication (ECOC - Valencia, Spain)

Patrick MOTTIER at Forum LED conference (Lyon, France).

Books

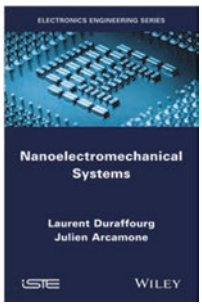

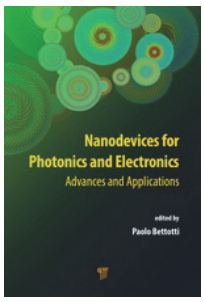

François SIMOENS, 'Cameras' chapter of the '*Handbook of Terahertz Technologies: Devices and Applications'*, edited by Ho-Jin Song & Tadao Nagatsuma, published by CRC Press

Laurent DURAFFOURG and Julien ARCAMONE edited the book "*Nanoelectromechanical Systems*" published by ISTE, WILEY, also in French with ISTE editions.

Badhise BEN BAKIR, Corrado SCIANCALEPORE, Antoine DESCOS, Hélène DUPREZ, Damien BORDEL and Sylvie MENEZO with a chapter in the «*Nanodevices for Photonics and Electronics: Advances and Applications*" book published by CRC Press

01

INFRARED IMAGING
Cooled HgCdTe and Microbolometers

- IR quantum imaging
- Low dark current HgCdTe detectors: SWIR, LWIR
- Avalanche HgCdTe photodiodes (APD)
- Small pitch, hybridization, optics, cooled detectors
- Microbolometer THz imaging
- IR presence sensor

The route to ultra-fine pixel pitch quantum IR detectors

Research topic: IR quantum imaging

O. Gravrand, F. Boulard, A. Ferron, G. Badano, S. Bisotto, J. Berthoz

Abstract: Future high performance IR imaging devices will probably require very small pixel pitches, of the order of the wavelength or below. Indeed, in tactical configuration (MW or LW with ambient temperature targets), the identification range would strongly benefits of some spatial oversampling. However, the range improvement highly depends on the fine pitch focal plane array features: will the modulation transfer function (MTF) stay optimum, even for very small pixel pitches? This gain in identification range calls for large integration times, therefore large integration capacitances. Will we be able to fit such large well fills in such a small area? A lot of questions have to be taken into account.

Context and Challenges

High performance tactical IR optronic systems are very concerned with the identification range. Basically, this range is the distance at which a given target may be identified with a relatively low error rate, before any tactical decision. However, lateral diffusion of photogenerated carriers in the photodiode array is a source of modulation transfer function degradation when the pixel pitch approaches the minority carrier diffusion in the absorbing materials, mainly HgCdTe (MCT). This issue has to be addressed for future fine pixel pitch tactical systems.

The need for modelling

In this context, modelling appears as a very useful approach for the optimization of photodiode MTF. A strong effort has thus been carried out within DEFIR common lab between LETI and Sofradir. Using 3D finite element modelling (FEM), the pixel MTF is reliably estimated (see figure below) for different pixel pitches (from 30 to 15µm), taking into account diode geometry and electrical properties of the absorbing material. In this latter case, the diffusion length (related to carrier lifetime) is of utmost importance for future systems has it determines the ability of the detector to operate at high temperature (highly desirable for future portable systems).

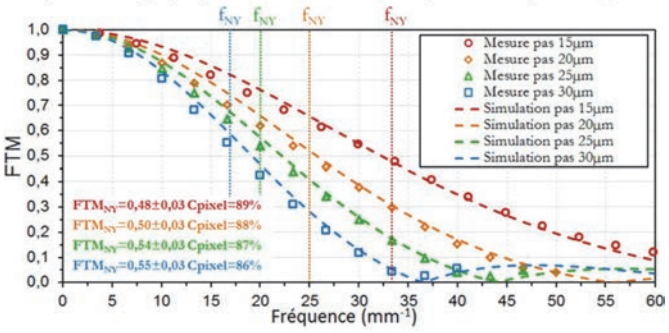

Modelling and experimental results for different pixel pitches planar structures with large diffusion length (20µm) suitable for high operating temperature

Going to very small pixel pitches

This approach has then been further used in the optimization of smaller pixels. Next figure shows the strong improvement obtained on 10µm pitch planar pixels, which are the next generation of focal plane array to be produced by Sofradir. Simulations showed first that a given parameter (hidden in the figure) was the parameter driving the MTF of planar small pitch photodiodes. Following MTF measurement showed a significant improvement of pixel MTF at Nyquist frequency.

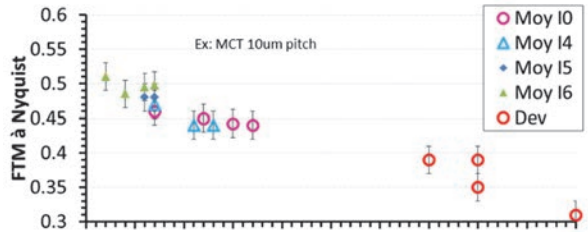

MTF Optimization of 10µm pixel pitches MCT arrays

Perspectives: Change the pixel structure?

However, 10µm pixel pitch is not the ultimate limit. The ultimate goal would be closer to 5µm for retinas operating in the MWIR range. To investigate such ultra fine pixels pitches, we probably need to totally rethink the pixel design, investigating planar photodiode as usuall, but also mesa structures where the lateral diffusion of photogenerated carrier is impeded by the etching of deep mesa trenches in the inter pixel space. Such a structure appears seducing on first seigth to mitigate MTF degradation for small pixel pitches, but mesa wall passivation has to be taken into account, as well as the quantum efficiency (QE) degradation due to the loss of absorbing material in the mesa trench. A last structure interesting for ultra small pixel pitch is the vertical photodiode shown in the last figure. In this case, the photodiode geometry allows an optimization of the self confinement by neighbooring pixel thus optimizing the resulting MTF.

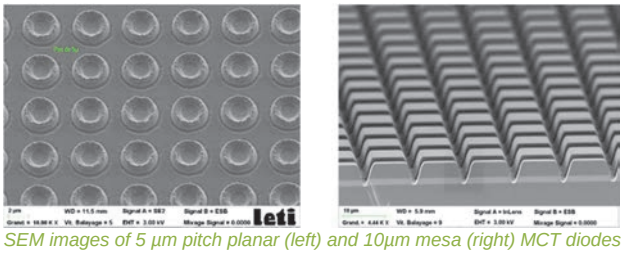

SEM images of 5 µm pitch planar (left) and 10µm mesa (right) MCT diodes

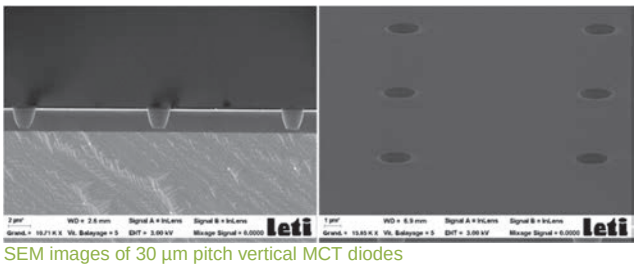

SEM images of 30 µm pitch vertical MCT diodes

Related Publications:
[1] Gravrand et al (2015). Ultra fine pixel pitch quantum IR detectors. SPIE Photonics West, Invited Paper..
[2] Berthoz et al. (2015). Modeling and Characterization of MTF and Spectral Response at Small Pitch on Mercury Cadmium Telluride. JEM, 44(9), p3157
[3] Berthoz, J. (2016). Caractérisation et modélisation par éléments finis des performances des détecteurs infrarouges refroidis à petits pas. Thèse.

Low dark current p-on-n MCT detector in long and Very long wavelength infrared

Research topic: IR Space applications, HgCdTe detectors, LPE heterojunction, VLWIR detector

C. Cervera, N. Baier, O. Gravrand, L. Mollard, C. Lobre, G. Destefanis, J.P. Zanatta, O. Boulade*, V.Moreau* (* CEA Saclay- IRFU, Gif sur Yvette, France)

Abstract: we present recent developments done at CEA-LETI Infrared Laboratory on processing and characterization of p-on-n HgCdTe (MCT) planar infrared focal plane arrays (FPAs) in LWIR and VLWIR spectral bands. This technology presents lower dark current and lower serial resistance in comparison with n-on-p vacancy doped architecture and is well adapted for low flux detection or high operating temperature. This architecture has been evaluated for space applications in LWIR and VLWIR spectral bands with cutoff wavelengths from 10µm up to 17µm at 78K. Innovations have been introduced to the technological process to form a heterojunction with a LPE growth technique. The aim was to lower dark current at low temperature, by decreasing currents from the depletion region. Electro-optical characterizations on p-on-n photodiodes have been performed on QVGA format FPAs with 30µm pixel pitches.

Context and Challenges

For some specific space applications with ultra-low flux conditions in long wavelength band, requirements in terms of dark current are particularly high. In such conditions, detectors have to be operated at very low temperature to lower the dark current at maximum. At low temperatures, dark current may not be limited by carrier diffusion regime. Depletion current in the junction may limit dark current, as it varies slower with temperature than diffusion current. These current limiting regimes vary as for diffusion and as where for depletion (typically with for generation-recombination current). To overcome this issue, a specific process, called bandgap widening, has been developed and tested. It aims at making a heterojunction with LPE process. Cadmium concentration is adapted along the layer thickness so that the junction is placed in material with higher bandgap than the active layer. The higher the bandgap at the junction is, the lower the depletion currents will be. Thus dark current will remain dominated by diffusion current at lower temperature.

Main Results

One epitaxial layer has been manufactured with the standard p-on-n process and serves as a reference. The cutoff wavelength has been determined with a spectral response measurement and is equal to 11.6µm at 78K. One other epitaxial layers were made using the heterojunction process. The cutoff wavelength is 11.7µm at 78K. Dark current density evolution with temperature is presented in 1 for FPAs respectively made with standard p-on-n process and bandgap widening process. Dark current evolutions appear to be identical from 80K to 40K, where the dark current is only limited by diffusion regime. Below these temperatures improved process exhibits dark current five times lower than standard process. The dark current gain allows to meet the space application requirements at 30K and not at 40K as expected. The explanation is that depletion current is not the main limiting dark current regime at low temperature in these specific conditions (long cutoff wavelength), diffusion current shifts to other kind of currents. It may be in the present case tunneling effect as photodiode reverse bias voltage plateau decrease with temperature. At very low temperature, tunneling effects may be dominant even at low bias.

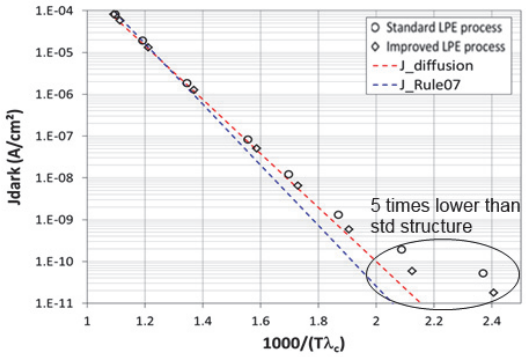

Figure 1 : Dark current density evolution for standard and heterojunction process. Experimental points are compared to Rule seven and a diffusion-depletion model.

The second part of this paper focus on preliminary results obtained in very long-wavelength IR detectors (VLWIR), with cutoff wavelength >15µm. A detector run has been manufactured, with higher cutoff wavelength to evaluate the robustness of the technology. At 40K, cutoff wavelength is equal to 19.7µm. Dark current measurements, as a function of bias voltage have been performed. Reverse voltage plateau decreases with the temperature due to strong tunneling effects (narrow bandgap). However, at intermediate temperatures, shunt resistance reaches a peak high enough to grant a proper bias of photodiodes and thus good conditions for FPA characterization. The values can be compared to Rule07 law at the highest temperatures, but tend to be greater at lower temperatures, with a factor slightly above 7 at 50K. This is mainly due to the tunneling effect as chosen bias to extract dark current is too high. However, it highlights the good performances of these photodiodes with such high cutoff wavelength.

Perspectives

We are now working to improve this new technological process to meet the space applications needs in terms of dark current and of operating temperature. In addition this kind of hetero-structure will be adapted to operate in SWIR and MWIR ranges.

Related Publication:
Cervera, C., Baier, N., Gravrand, O., Mollard, L., Lobre, C., Destefanis, G., Moreau, V. Low-dark current p-on-n MCT detector in long and very long-wavelength infrared. Proc. SPIE, 9451, 945129. doi:10.1117/12.2179216 (2015)

Ultra-low-dark current p-on-n MCT detector in short-wavelength infrared for space applications

Research topic: IR Space applications, HgCdTe detectors, LPE heterojunction, VLWIR detector

C. Cervera, O. Boulade*, O. Gravrand, C. Lobre, F.Leguellec, JL.Santailler, E.Sanson, P.Ballet, J.P. Zanatta, V.Moreau*, B.Fieque**, and P.Castelein**.
(* CEA Saclay- IRFU Gif sur Yvette, France and ** SOFRADIR, Veurey-Voroize – France)

Abstract: we present recent developments performed at CEA-LETI Infrared Laboratory on processing and characterization of p-on-n HgCdTe (MCT) planar infrared focal plane arrays (FPAs) in SWIR spectral band for the astrophysics applications. These FPAs have been grown using both liquid phase epitaxy (LPE) and molecular beam epitaxy (MBE) on a lattice matched CdZnTe substrate. This technology exhibits lower dark current and lower serial resistance in comparison with n-on-p vacancy doped architecture and is well adapted for low flux detection or high operating temperature. This architecture has been evaluated for space applications in LWIR and VLWIR spectral bands with cutoff wavelengths from 10µm up to 17µm at 78K and is now evaluated for the SWIR range. The metallurgical nature of the absorbing layer is also examined and both molecular beam epitaxy and liquid phase epitaxy have been investigated. Electro-optical characterizations have been performed on individual photodiodes from test arrays, whereas dark current investigation has been performed with a fully functional ROIC dedicated to low flux operations.

Context and Challenges

Space-based observatories for astrophysics are very demanding in ultra-low flux detection in the IR spectrum. Such low flux levels represent the detection of a few photons only during long integration times (typically 1e-/s during several minutes) and therefore require ultra-low dark current photodiodes coupled to a very high performance ROIC stage in terms of noise and leakage. In the frame of its NIR-SWIR roadmap, ESA is funding the development of a 2Kx2K 15µm pitch array with the aim of reaching the level of electro-optical performances that are required for astrophysics missions such as EUCLID. The main objective is to reach a very low dark current (close to 0.1e-/s) with a large Quantum Efficiency (QE>70%) operating detectors in the 100K temperature range.

Main Results

Two epitaxial layers have been manufactured one with a MBE process and another with LPE process. The cutoff wavelength has been determined with a spectral response measurement and is equal to 2.1µm at 78K for both layers. These layers have been hybridized on a 512x640 source follower per detector readout circuit (ROIC) which has been designed with 15µm pitch. Then low flux characterizations have been carried out at CEA-SAp at low temperature.

The dark current was measured at all temperatures from 40 to 160K in steps of 10K. All measurements were performed in nondestructive readout mode (FUR) with a time sampling of 1.4s from 40 to 160K. For each diode, the dark current is measured as the slope of the evolution of the output signal with time. Figure 1 shows dark current measurement obtained at 100K. After subtraction of the glow from the ROIC these results are in good agreement with the ESA requirements (0.1e-/s) and no strong differences appear between MBE and LPE layers.

For low flux applications a high quantum efficiency is necessary to obtain a large signal from different sources. Figure 2 represents quantum efficiency for MBE and LPE. No difference is seen between LPE and MBE material, QE values are close to 80%. The sharp transition of the response at 0.8µm is only due to the CZT substrate which is not removed on the PV meaning a cut-on frequency as low as 0.4µm can be reached if CZT substrate can be removed. All results highlight the very good quality of p-on-n technology for astrophysics systems, with an excellent dark current and high QE values.

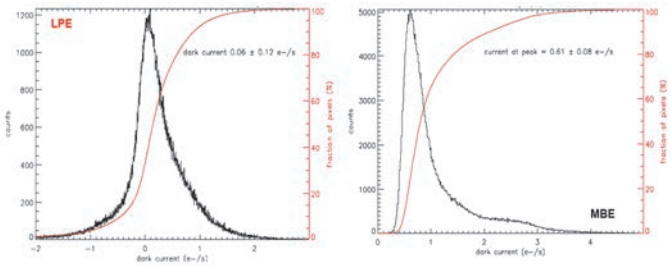

Figure 1 : Distribution of dark currents estimated at 100K.

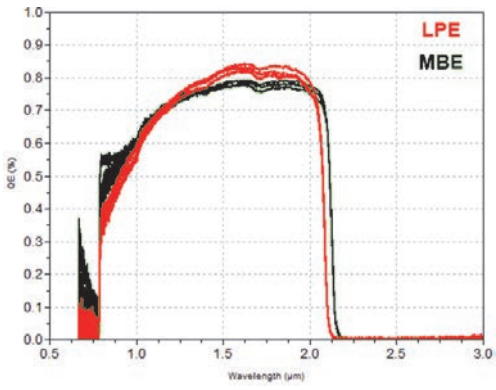

Figure 2 : Spectral QEs measured on test chips 15µm pixels from both LPE and MBE layers.

Perspectives

Further development will now focus on the scaling of the FPA to larger devices, up to 2k x 2k, in order to address the real need in astrophysics imaging. Furthermore, additional efforts are mandatory in order to mitigate the ROIC glow and get access to the available full performance given by the MCT photodiodes.

Related Publication:

Cervera, C., O.Boulade, O.Gravrand, C.Lobre, F.Guellec, E. Sanson, P. Ballet, JL. Santailler, V. Moreau, JP. Zanatta, B. Fieque and P. Castelein, Journal of Electronics materials (under review, 2016), Special Issue Workshop on the Physics and Chemistry of II-VI Materials, paper number: JEMS-D-16-00529 (2015)

Response time and sensitivity modeling of HgCdTe avalanche photodiodes for free space optical telecommunications

Research topic: Photodetection, avalanche photodiodes, free space optical telecommunications

J. Rothman, J Abergel and G Lasfargues

Abstract:
The sensitivity expected in high gain and bandwidth HgCdTe APDs made at Leti have been calculated as a function of the active optical area and operating temperature. A gain in sensitivity of close to two order of magnitudes is expected in large area HgCdTe APDs operated at temperatures close to 300 K. Such performance could be a key enabler in tomorrow's high data-rate satellite telecommunication networks.

Context and Challenges

The access to high data rate internet even at remote locations is becoming a fundamental stake of equity in today's societies. Such all-territory high data-rate coverage will require the development of new space based free space optical (FSO). One of the main challenges in the development of such links is the detection of the faint transmitted optical signal using emitters and telescopes with a reasonable size and power consumption. The optical amplifiers, such as EDFAs, that are currently used in fiber based networks, are currently based on the uses single mode fibers into which it is not possibly to couple the remaining light with a good efficiency.
HgCdTe APDs are particularly promising in this emerging field as they offer a high linear gain associated with a low excess noise factor that enables to detect the optical with close to zero loss in information. The present communication discusses the sensitivities that can be achieved in such APDs depending on the optically active area and operating temperature.

Main Results

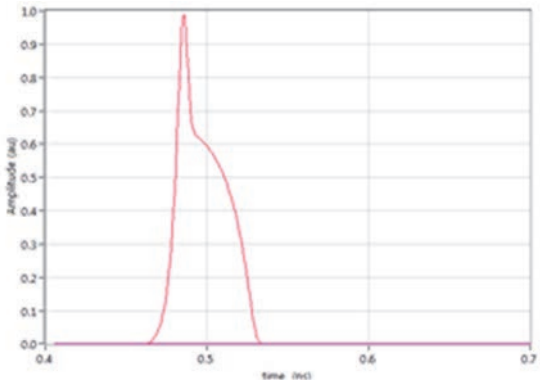

Fig.1: Estimation of the response time in a HgCdTE APD with λ_c=2.7 µm at 300 and a junction width of x_j=0.8 µm and v_e=3.5x10^6 cm/s, v_h=1.9x10^6 cm/s. The width of the response is FWHM< 50 ps and the corresponding BW = 9 GHz.

The use of HgCdTe APDs for telecom applications depends in first order on the capacity to achieve a sufficient bandwidth in theses detectors. In particular, a minimum bandwidth of 10 GHz will be needed to enable a high speed Tbit/s link using wavelength division multiplexing (WDM). At present, no specific effort have been dedicated to the optimization of the bandwidth (BW) in HgCdTe APDs. The response time can however be calculated from the estimations of the drift velocities of the carriers during the avalanche multiplication, reported in [1]. The estimation shows that bandwidths in excess of 9 GHz can be achieved in such APDs, when the contribution from carrier collection and RC are negligible. The modeled response time of such HgCdTe APD is reported in figure 1

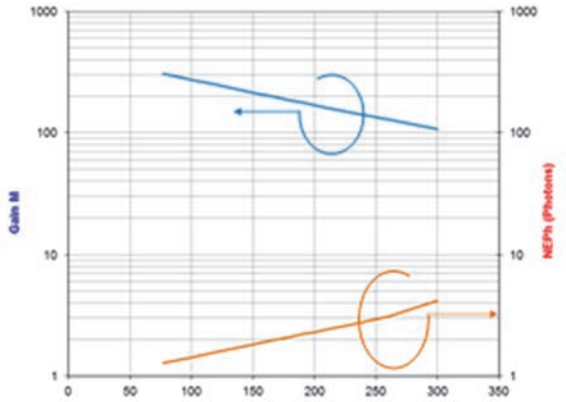

Fig. 2: Modelled APD gain and sensitivity (NEPh) towards T (°K) of 15 µm with λc=2.8 µm HgCdTe APD operated at fixed bias (17.5 V) and coupled with a 10 GHz bandwidth TIA with an equivalent input current noise density of 10 pA/$\sqrt{}$Hz

The sensitivity of high bandwidth photodiode is strongly limited by the noise induced by the amplifier circuit used to generate a signal that is sufficiently strong to be sampled and decoded without additional loss of information. The avalanche gain reduces the impact of the amplifier noise as long as the noise induced by the diodes dark current does not give a dominating contribution to the noise. The sensitivity of HgCdTe APDs, expressed as the equivalent fluctuation of photons detected during an observation equal to 1/2BW, have been modeled using analytical expressions of the dark current that has been calibrated using experimental data. The calculations shows that sensitivity can be improved with close to two order of magnitude compared III-V APDs, reaching equivalent input noises of 4 photons, corresponding to a an input power of -50dBm, for operating temperature between 250 and 300 K for detector sizes ranging from 200 µm to 15 µm, respectively. Such high sensitivities would play a fundamental role in enabling high data-rate optical data transfers in space.

Perspectives

The optimization of HgCdTe APDs device architecture and processing should enable 10 GHz BW. The development of such detectors is a key to the deployment of a new space based optical telecom network and it will be one of the main challenges during the next years for this technology

Related Publications:
[1] J. Rothman, et al., J. Electrons Mater., 43, 2947 (2014)
[2] J. Rothman, et al., Proc. SPIE (2015)

Terahertz real-time imaging with uncooled arrays based on antenna-coupled bolometers or FETs

Research topic: Terahertz, Imaging, Bolometer, Field-Effect Transistors

F. Simoens, J Meilhan J, J.A Nicolas, N Monnier, J Lalanne-Dera, J.L Ouvrier-Buffet, A Hamelin, S Gidon and B Delplanque

Abstract: Sensitive and large-format TeraHertz Focal Plane Arrays (FPAs) integrated in compact and hand-held cameras that deliver real-time terahertz (THz) imaging are required for many application fields, such as Non-Destructive Testing (NDT), security, quality control of food and agricultural products industry. Two technologies of uncooled THz arrays that are being studied at CEA-Leti, i.e. bolometer and CMOS Field Effect Transistors (FET), are able to meet these requirements. State-of the art sensitivity has been demonstrated by the prototyped bolometer-based camera operated in video mode. New ROIC CMOS architectures for THz FET arrays are being under tests with promising performance.

Context and Challenges

The unique properties of Terahertz (THz) radiation open the way to promising applications in numerous interdisciplinary fields –such as non-destructive testing, homeland security, quality control of food and agricultural products. Many of these applications require real-time imaging. A growing number of THz cameras are now available on the market or under development in research laboratories worldwide

A wide variety of technologies is investigated (refer to [1] that reviews THz camera technologies) but few of them integrate large-format (i.e. many-pixel) focal plane arrays and, like any digital camera, operate in video-mode recording streams in real-time without the need for raster scanning. Moreover the spread of THz imaging applications would be greatly increased by the availability of affordable, compact, easy-to-use and highly-sensitive cameras.

CEA-Leti is being developing two technologies of uncooled THz arrays [2] that are good candidates to meet the requirements of this emerging market:

1- Owing to its state-of-the-art know-how in thermal infrared bolometer sensors, CEA-LETI has initiated in 2005 the development of THz sensors based on the tailoring of IR microbolometer to THz waves. State-of the art sensitivity has been demonstrated by the prototyped camera operated in video mode.

2- A few years later, in collaboration with the French University of Montpellier, Leti initiated the study of THz arrays based on CMOS Field-Effect Transistors (FET). Since 2011, the Leti analog design group has designed and tested very promising new ROIC CMOS architectures for THz FET arrays.

Bolometer-based THz video camera

The key innovation of the Leti patented THz bolometer architecture relies on the separation between the two main functions of such sensors, i.e. the electromagnetic absorption and the thermometer. The absorption of THz radiation is performed by antennas and an optimized quarter-wavelength cavity located under the antennas. Crossed quasi double-bowtie antennas, named 'CC' and 'DC' (refer to Fig 1, left), are coupled to the central bolometer micro-bridge and are resistively loaded.

This two-storied antenna architecture permits the tuning of the optical coupling of both polarizations separately and with no mutual interferences. Moreover, antennas sizes and shapes can be chosen independently from the bolometric device to match the illumination characteristics, and in particular the frequency range.

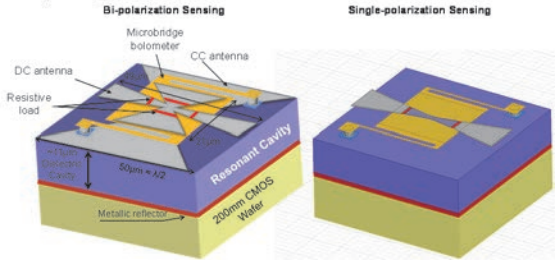

Fig1: pixel architecture versions for bi (a) or single (b) polarization sensing

Extensive work of modelling – FEM or FDTD electromagnetic 3D simulations – has been carried out in order to validate the design tools through comparison with experimental tests [4].

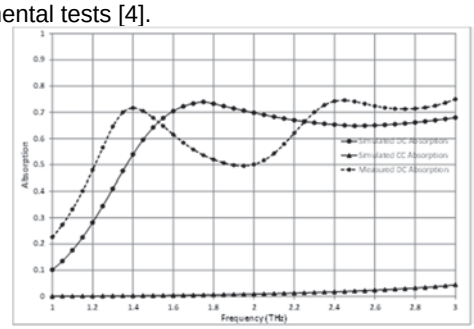

Fig2: Measured (dotted) and simulated (continuous) absorption of single DC polarization antenna bolometer. No absorption in the CC direction is observed.

A particular design with one of the 2 bow-tie antennas being suppressed has been studied (Fig 1, right). A single antenna design – keeping here the so-called DC bow-tie antenna – has been implemented in a 3x3 pixel micro-array and spectral response measurements of the device have been performed. Measurements exhibit overall consistency with simulation: they show a significant broadening of absorption that is consistent with single element bowtie antenna frequency behavior while orthogonal polarization (CC direction on Fig 2) has null absorption.

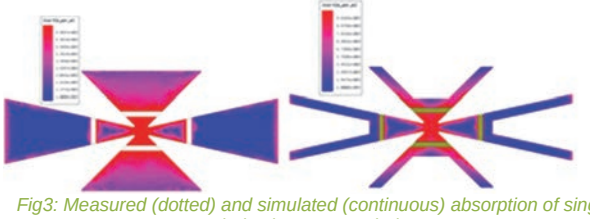

Fig3: Measured (dotted) and simulated (continuous) absorption of single DC polarization antenna bolometer.

An alternative design that provides both fast response time and cross-polarization sensibility has been modelled: it consists in a novel antenna structure where most of the central metallic part is removed (Fig 3.) so that its thermal capacitance is reduced. Thanks to this structure thermal time constants close to 20ms can be reached, that is in the range of state of the art IR bolometers at similar pitch.

Fig4: 320x240 pixel array-based video THz camera prototype

320x240 arrays with 50µm pitch pixels have been designed, processed and tested. A dedicated CMOS application-specific integrated circuit (ASIC) has been developed by CEA-Leti teams to ensure low-noise video data stream. Chips have been integrated in a compact video camera housing (Fig. 3) for diverse imaging demonstrations.

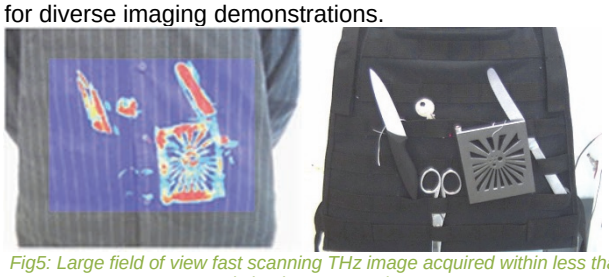

Fig5: Large field of view fast scanning THz image acquired within less than 10 seconds by the scanner demonstrator

Fast scanning of large field of view of opaque scenes has been achieved in a complete body scanner prototype. Each individual image acquired in real-time corresponds to a 40x60 mm² surface at the scene level. In order to cover the size of a chest, one mirror is successively moved in order to compose a 5x5 tiled array of individual images. A human trunk of a typ. 20x30 cm² surface has been successfully scanned in less than 10 seconds (Fig. 5). Metallic and ceramic objects can be identified even when concealed under a shirt.

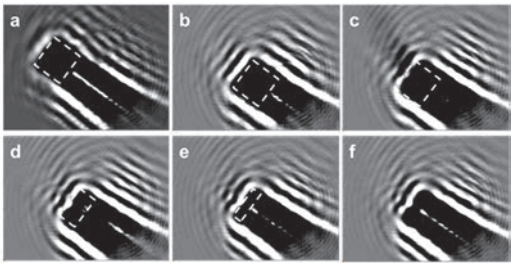

Fig 6: Images sequence of the pipette nozzle dropping its water content (the dotted rectangle shows the water droplet estimated position)

Recently a very simple shadowgraph optical system has been set-up at the output of a CO2 pumped molecular laser emitting at 2.5 THz. Various objects have been manually moved within the collimated part of the propagating THz beam and imaged with the bolometer array (Fig. 6). The acquired videos have demonstrated the robustness of the camera use [2].

CMOS FET-based THz arrays

Leti has especially worked on the reduction of the noise by implementing signal processing techniques within the pixel itself. In order to overcome 1/f noise, the input THz signal is modulated at a frequency fmod at the source level, moving the drain-source output voltage of the pixel from DC to fmod. Much like lock-in detection techniques, the transposition of the image signal to an upper frequency band allows a selective filtering of the noise, especially the prevalent 1/f noise.

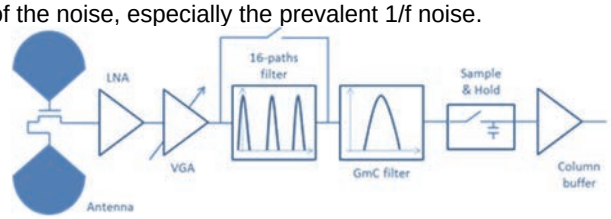

Fig6: Pixel block diagram

To achieve this selective filtering, Leti presented a specific in-pixel readout architecture based on N-path filters depicted in Fig. 6. A test pixel has been embedded in a CMOS circuit allowing the fine characterization of the readout chain performances. The resulting NEP values are respectively 1.6 nW at 200 GHz, 533pW at 270 GHz and 732 pW at 600 GHz. At the cost of an increase of the power consumption, thanks to the combination of in-pixel low dispersion amplification and selective filtering with a modulation of the THz source, the sensitivity is significantly improved in comparison to state-of-the art works.

Perspectives

Leti has developed a unique bolometer-based THz pixels, where antennas and a resonant cavity tuned for THz sensing are key elements ([3]). In addition to state-of-the-art sensitivity demonstrated in video mode, this architecture provides high flexibility in pixel design and THz array functionalization.

In the FET-based THz field, innovative CMOS read-out- circuit design has been designed and tested. The studied architecture takes advantage of the large pixel pitch to enhance the flexibility and the sensitivity: an embedded in-pixel configurable signal processing chain that dramatically reduces the noise.

These arrays have been extensively characterized and also integrated in several active imaging set-ups for demonstration of their capabilities both in reflection and transmission configurations. Video sequences at 100 frames per second using our 31x31 pixels prototyped 2D FPAs have been tested. Thanks to its higher technological maturity, the 320x240 THz bolometer array has been integrated in a complete system to demonstrate fast scanning of large field of view of opaque scenes.

Both technologies are fully compatible with standard CMOS microelectronic equipment and therefore benefits from the maturity of the silicon technology. The combination of these features meets the criteria of low cost and low SWAP (size, weight and power) that any commercial camera has to target. Future works will target performance improvement and development of customized sensors meeting industrial application-driven specifications, like extended spectral range, polarization dependence or compactness requirements.

Related Publications:
[1] Simoens F., 'THz cameras' chapter of the Handbook of Terahertz Technologies: Devices and Applications', edited by Ho-Jin Song & Tadao Nagatsuma, by Pan Stanford, ISBN 9789814613088, April 15, (2015)
[2] Simoens F., Meilhan J., Nicolas J.A., 'Terahertz Real-Time Imaging Uncooled Arrays Based on Antenna-Coupled Bolometers or FET Developed at CEA-Leti', J. Infrared Millim. Terahertz Waves, Vol. 36, pp. 961–985, (2015)
[3] Simoens F., Meilhan J., 'Terahertz real-time imaging based on uncooled antenna-coupled bolometer arrays developed at CEA-LETI: review and perspectives', invitation-only presentation at the international Symposium on Frontiers in THz Technology (FTT) 2015 at Hamamatsu, Sept (2015)
[4] Meilhan J., Ouvrier-Buffet J.L., Hamelin A., Delplanque B., and Simoens F., 'Recent advances in modelling and characterization of uncooled antenna-coupled bolometer arrays', 40th International Conference on Infrared, Millimeter, and Terahertz Waves (IRMMW-THz), Hong-Kong, China (2014)

Uncooled infrared microbolometer presence sensor

Research topic: microbolometer, sensor, lighting

L. Alacoque, S. Martin, W. Rabaud

Abstract: Leti has developed a new solution for lighting applications, for presence detection, thanks to an innovative readout circuit with 128 RISK processors included inside the infra-red bolometer focal plane array. Low level and high level detection algorithms have also been created and part implemented inside the readout circuit.

Context and Challenges

The EnLight project looked for greatly improved energy efficiency and user comfort in lighting applications. The closer the relation between the user and his requirements in terms of light provided in space and time, the better the comfort. These demands were fulfilled by advanced sensors and EnLight's distributed rulesbased intelligence concept. Various physical parameters are important and need to be measured to allow proper decision-making such as occupancy, and position of people in a room.

Main Results

In the frame of the EnLight project a new kind of presence sensor was developed by Leti. It is based on a thermal IR (Infrared) sensor that is able to detect presence under arbitrary lighting conditions (daylight, night…). Detection considers both still and moving people. This development fills the gap between the low price-low pixel size detectors (PIR, thermopiles…) and the high price-high pixel size IR imagers (µ-bolometers).

The new IR µbolometer based presence sensor was developed on two parallel tracks: the first one is the development of low complexity detection algorithms (low-level and high-level), and their implementation on the EnLight demonstrator that was specifically developed for the project. In this prototype the detection algorithm provides semantic descriptors to the output, preserving intrinsic privacy. The low-level algorithms were designed to avoid thermo-electrical coolers. They enable shutterless operation of the sensor with fixed pattern noise removal. They are robust to environmental temperature variation, and self-commissioning. The high-level algorithms allow very low complexity target detection: the result of the detection process is provided at the output by semantical descriptors. The result of such detection is illustrated in Figure 4, where each square stands for the detection of a person through a dedicated android application developed for the project.

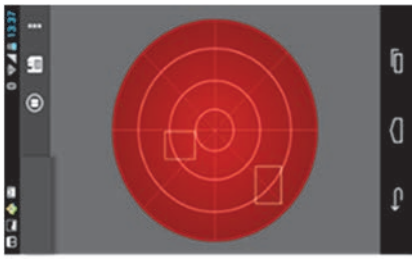

Results of the detection process; each square stands for a detected person.

The second track was on the development of a specific integrated circuit. The application specific integrated circuit for autonomous low-cost, low-power steady presence sensing and counting was successfully fabricated on a general-purpose 130nm technology from Altis semiconductors. The wafers were post-processed in the MINATEC clean-room facility for the implementation of IR bolometers MEMS. The integrated circuit with the IR bolometers built on top forms the sensor focal plane array. The latter is a 128x128 pixels matrix with 128 SIMD RISC processors and 128 application-specific ADCs (patented). A general purpose instruction set is implemented inside the processors which allows a broad range of applications and reduces system cost. Moreover, on-chip processing avoids image transfer and saves power.

The circuit proved its ability to perform privacy-compliant fully-digital thermal image acquisition and on-the-fly processing. Benchmarking with latest commercial products and articles in the literature show a power consumption reduction of more than ten times using this new dedicated integrated circuit (around 0.5µW/pixel).

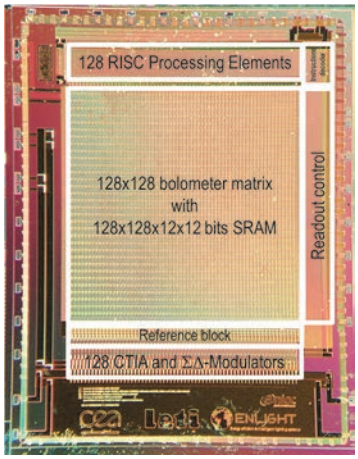

The 128x128 pixels application specific integrated circuit for autonomous low-cost, low-power steady presence sensing and counting.

Perspectives

We have demonstrated the potential of such a new solution for lighting applications. This potential should now be turned into a true prototype to validate it against standard solutions.

Related Publication:
LED Professional Review magazine_2015_ #48 (p66-105)

02

OPTICAL ENVIRONMENTAL SENSORS

- Gas detection
- Non-dispersive IR sensors
- Integrated photo-acoustic sensors

Upgrading infrared thermal emitters with plasmonic metasurfaces

Research topic: gas sensing, MEMS, membrane, black body, plasmonics, metamaterials

A. Lefebvre, D. Costantini*, J.J Greffet*, H. Benisty*, S. Boutami
(* Institut d'Optique, CNRS, France)

Abstract: Micromembrane thermal emitters are interesting infrared sources for low cost and low consumption gas sensors. We developed a new approach based on plasmonic metasurfaces to make these sources, intrinsically non dispersive, monochromatic and directive. The goal pursued consists in increasing the efficiency of these sources that is their electro-to-optic yield. This approach paves the way to low cost and even less consuming sources, for highly autonomous sensors.

Context and Challenges

Micromembrane thermal infrared emitters are less powerful than quantum cascade lasers, but much cheaper, and thus useful for low cost, low consumption, gas sensors. The potential of such membranes for gas sensing applications has already been demonstrated, most gases showing absorption fingerprints in the mid infrared [1]. To make them even more attractive for autonomous device, we have investigated the implementation of plasmonic metasurfaces on such thermal emitters, to tailor their emissivity. Although it is physically impossible to overcome blackbody radiance, one can however annihilate the emissivity in useless wavelengths or emission angles, regarding the gas under study and the afferent optical system. The restriction of radiative emission to only useful radiation reduces the channels by which the membrane can cool down, which reciprocally reduces the amount of current and thus consumption needed to bring it to operating temperature, while maintaining the same optical efficiency.

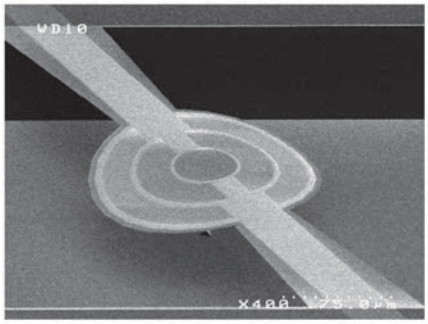

Figure 1: SEM image of a micromembrane infrared thermal emitter [1]

Main Results

We demonstrated the potential of such metasurfaces on monolithic wafer demonstrators. These metasurfaces consist in metal-isolant-metal (MIM) periodic nanostructures, which support resonant gap plasmonic mode, at specific wavelength depending on their lateral width [2]. We have shown that, by a proper choice of the period, it is possible to control the emission diagram of such structures, though generally known to be isotropic, by perturbing the critical coupling condition [3-5]. This approach will be also demonstrated using fully CMOS-compatible process, at full wafer-scale.

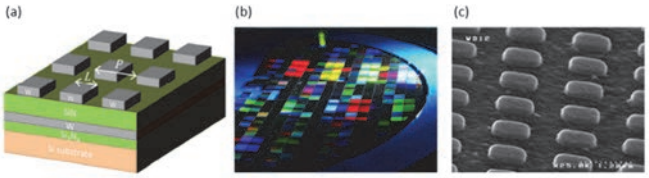

Figure 2: (a) Metasurface picture; (b) 200mm Si wafer with 5x5mm^2 dies of MIM arrays of different periods; (c) SEM image of a MIM array

Experimental emissivity showed a behavior comparable to simulated absorption, in accordance with Kirchoff's law. The infrared thermal emission is quasi-monochromatic, suited to CO_2 detection, regarding broadband black-body radiation envelope, and is also quasi directional, restricted mainly to quasi-normal emission angles, that can be collected by an optical system.

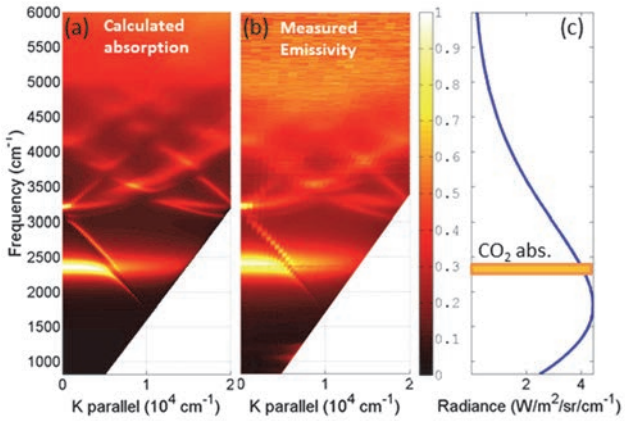

Figure 3: (a) Calculated absorption for the metasurface; (b) Measured emissivity when heating at 600°C; (c) blackbody radiation vs CO2 absorption band (λ=4.26µm)

Perspectives

Next step will consist in implementing these nanostructures on micromembranes, for integration in highly autonomous low cost gas sensors. These developments are performed in the frame of startup Elichens activies, developing gas sensors for monitoring air quality.

Related Publications:
[1] P. Barritault, M. Brun, S. Gidon, S. Nicoletti, « Mid-IR source based on a free-standing microhotplate for autonomous CO2 sensing in indoor applications ", Sensors and Actuators A: Physical 172, 379– 385 (2011).
[2] A. Lefebvre, S. Boutami, J.J. Greffet, H. Benisty, "Optimization of a radiative membrane for gas sensing applications", Proceedings of SPIE, 9141, 91410G, Photonics Europe, Brussels (2014); Best student paper award.
[3] A .Lefebvre, D. Costantini, G. Brucoli, S. Boutami, JJ Greffet, H. Benisty, "Influence of emissivity tailoring on radiative membranes thermal behavior for gas sensing applications", Sensors and Actuators B-Chemical 213, 53-58 (2015).
[4] F. Marquier, D. Costantini, A. Lefebvre, AL Coutrot, I. Moldovan-Doyen, JP Hugonin, S. Boutami, H. Benisty, JJ Greffet, "Metallic metasurface as a directional and monochromatic thermal emitter", Proceedings of SPIE 9370, 937004, Photonics West, San Francisco (2015).
[5] D. Costantini, A. Lefebvre, A.L. Coutrot, I. Moldovan-Doyen, J.P. Hugonin, S. Boutami, F. Marquier, H. Benisty, J.J. Greffet, "Plasmonic Metasurface for Directional and Frequency-Selective Thermal Emission", Physical Review Applied 4, 014023 (2015)

SiGe AWG: towards multi-lambda source

Research topic: Integrated optics; Instrumentation, measurement and metrology; Infrared, gas sensors.

P Barritault, M Brun*, P Labeye, J-M Hartmann, F Boulila*, M Carras* and S Nicoletti.
(*MIRSENSE-centre NanoINNOV -Palaiseau- France)

Abstract: we present an Arrayed Waveguide Grating (AWG) based on a SiGe graded index waveguide platform, operating at 4.5 µm. The devices were specifically designed to work together with an array of Distributed Feedback Bragg Quantum Cascade Lasers (DFB-QCL) emitting at different wavelengths. The AWG enables to combine the different light sources into a single output.

Context and Challenges

Mid Infra-Red (mid IR) is particularly interesting in the field of spectroscopic gas sensing. Indeed, many gases present strong absorption lines in this spectral area. Moreover, the appearance of new mid IR laser sources such as Distributed Feedback Bragg Quantum Cascade Lasers (DFB-QCLs) permits the easy, and highly specific, detection of these gases by a simple absorption measurement. These sources present a high spectral purity (typically 10 MHz when used in continuous mode) and a high stability. However, their tunability is quite small (3 cm^{-1}), limiting the use of one laser for one gas. Given that, we propose, in order to tackle the issue of multi-gas sensing, to combine an array of DFB-QCLs, evenly spaced by steps of 3 cm^{-1}, with a wavelength multiplexer. The idea there is to obtain a tunable, monolithic, single output source. Wavelength tuning can be done either by changing the driving current of one DFB-QCL within its 3 cm^{-1} range of tunability, or by switching from one DFB-QCL to the next one. As an example, ideally, an array of 15 DFB-QCLs evenly spaced by 3 cm^{-1} steps when combined to an appropriately designed multiplexer, will yield a monochromatic light source, having the spectral purity of a single DFB-QCL but being tunable over a range of 45 cm^{-1}. We will now focus on the multiplexer, which is the topic of this article.

Main Results

We have developed a new waveguide platform based on SiGe graded index waveguides [1]. This material presents a wide transparency range from 3 µm to 8 µm and full compatibility with Complementary Metal Oxide Semiconductor (CMOS) processing. It allows the fabrication of single mode waveguides in the full transparency range. As a first proof of concept, we have thus fabricated an AWG working at 4.5 µm [2].

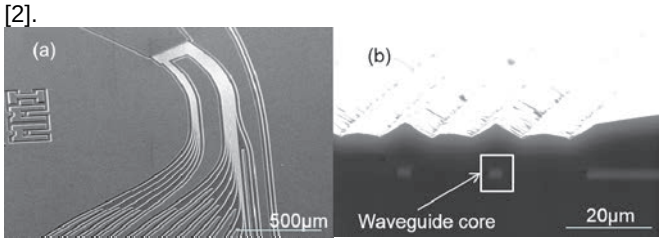

Fig. 1. (a) 3D SEM pictures of the AWG structures, details of the waveguide routing toward the AWG entrance. (b) Cross-sectional SEM picture of the AWG showing the core of the waveguides.

The core layer of the waveguide consists in a graded index SiGe layer grown by reduced pressure epitaxy where the Ge content is linearly increased from 0% to 42% and then decreased down to 0% in a quasi-triangular profile which is 3 µm thick. To define all the passive functions, the waveguides core is patterned in this layer by conventional photolithography and deep reactive ion etching processes. Fig. 1 shows 3D and cross-sectional Scanning Electron Microscopy (SEM) images of an AWG Multiplexer just after this step.

In order to characterize these AWG, we have also developed an experimental setup sketched in Fig. 2. The principle is to inject a broadband source, e.g. a Fabry Perot QCL (FP-QCL), in each input of the AWG and to spectrally analyse each output with a FTIR spectrometer.

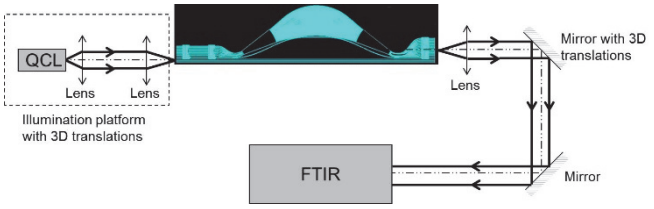

Fig. 2. Experimental setup used to characterize the AWG.

In Fig.3, we present an example of the spectrum recorded at the output of 9 adjacent exits when the broadband source is injected in a single input.

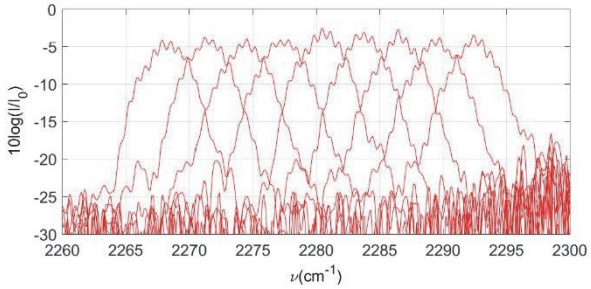

Fig. 3. Spectrum measured at the output of 9 adjacent exits.

Perspectives

Following this work, two other AWG, working at 5.65µm and 7.4µm, based on the same technological platform were developed and characterized with success. These realizations were followed by the creation of a start-up “Mirsense”. One of their up-coming products is the wide range monochromatic light source described above [3]. This work is done in a joined lab with our laboratory.

Related Publications:
[1] M. Brun, P. Labeye, G. Grand, J.-M. Hartmann, F. Boulila, M. Carras and S. Nicoletti, "Low loss SiGe graded index waveguides for mid IR applications," Opt. Express 22, 508–518 (2014).
[2] P Barritault, M Brun, P Labeye, J-Ml Hartmann, F Boulila, M Carras and S Nicoletti, " Design, fabrication and characterization of an AWG at 4.5 µm," Opt. Express 23, 26168–26181 (2015).
[3] M. Carras, G. Maisons, B. Simozrag, V. Trinite, M. Brun, G. Grand, P. Labeye and S. Nicoletti , "Monolithic tunable single source in the mid-IR for spectroscopy," Proc. SPIE 8631, 863113–7 (2013).

3D-printed Photo-acoustic cell for CO2 and CH4 gas measurement: toward compact and plug-and-play gas analysis

Research topic: mid-infrared, photoacoustic, spectroscopy, quantum cascade lasers.

JG Coutard, J Rouxel, O Lartigue, F Badets, L. Duraffourg and A Glière

Abstract: Photoacoustic cells are one type of optical sensors that can be used to detect trace gases. The photoacoustic spectroscopy technique is based on the absorption of photons by the molecules of interest and the subsequent creation of acoustic waves. It is extremely sensitive but the sensor bulkiness and cost prevent their use in applications where mass deployment is required. A trend towards miniaturization is thus engaged using available quantum cascade lasers in mid infrared region where many gases have their strongest absorption lines.

Context and Challenges

PhotoAcoustic Spectroscopy (PAS) is one of the most sensitive techniques used to monitor chemical emission or to detect gas traces [1]. In particular, in the Mid InfraRed (MIR), many gases of interest have their strongest absorption lines making the MIR PhotoAcoustic spectroscopy a high potential technique.

However the current PAS commercial sensors are bulky, expensive and complex. In the same time powerful MIR sources like Quantum Cascade Laser (QCL) become available for a large range of wavelengths, meaning gases. Our goal is to bring together those technologies to build an ultrasensitive detector on a small foot print - i.e. centimetric – and at low cost.

Main Results

Based on a Differential Helmholtz Resonator (DHR) design [2] we have developed and characterized, at bench level, our photo acoustic cell associated to QCL's.

The photo acoustic cell termed miniPA has been designed by modelling acoustic wave induced by MIR laser pulse absorption through finite element method [3]. It has led to the manufacturing of a stainless steel cell by direct metal laser sintering (DMLS). Moreover, we have developed a specific readout lock in amplifier board to cope with the aim of compactness and cost of the whole detection chain.

Figure 1: PhotoAcoustic cell featuring mems microphones,

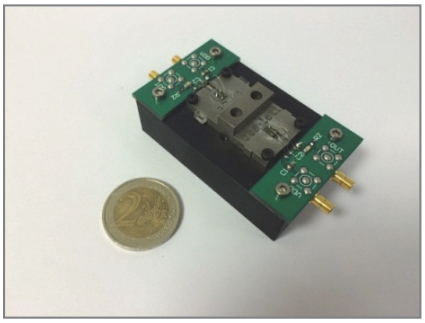

CaF2 windows and PCB to manage signal and power

Finally, we have built a complete functional detection chain on bench with QCL sources, miniPA cell, specific readout board and software.

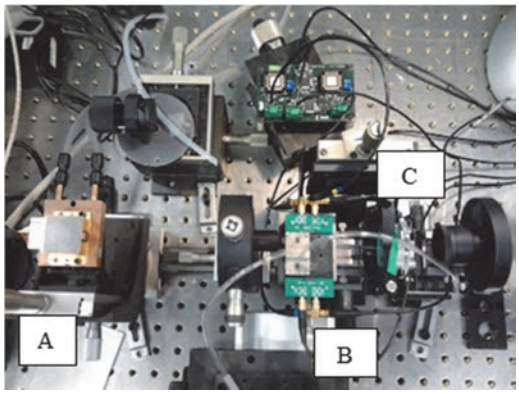

Figure 2: Test bench with QCL(A), miniPA(B) and readout board MIRIFIC (C).

We have assessed our detector on CO_2 and CH_4 using mirSense QCL's (see www.mirsense.com). For each gas, a frequency response and a calibration curve have been achieved. Limits of detection (LOD) largely beyond 1ppm have been demonstrated for the two gases at 2 kHz-acoustic resonance frequency. (LOD = 255 ppb and 96 ppb for CO_2 and CH_4 respectively).

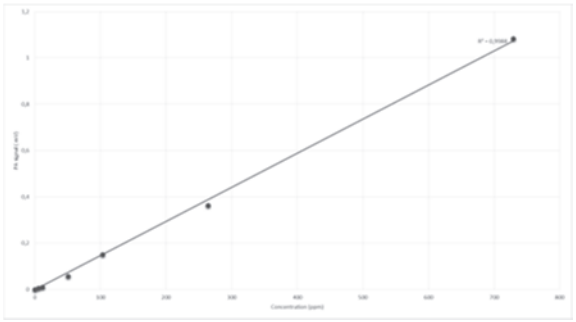

Figure 3: calibration curve for CO2 from 0 to 3000ppm. The LOD is 255ppb.

Perspectives

These results open the way to the integration of a compact high performance gas detector. In particular our work is now focused on the hybridization of QCLs on Si including a mini photo acoustic cell [4]. The full system is currently integrated in unique package with multigases detection capability.

Related Publications:

[1] A. Miklós, P. Hess, and Z. Bozóki, "Application of acoustic resonators in photoacoustic trace gas analysis and metrology," *Rev. Sci. Instrum.*, vol. 72, no. 4, pp. 1937–1955, Apr. 2001.

2] V. Zeninari, V. A. Kapitanov, D. Courtois, and Y. N. Ponomarev, "Design and characteristics of a differential Helmholtz resonant photoacoustic cell for infrared gas detection," *Infrared Phys. Technol.*, vol. 40, no. 1, pp. 1–23, Feb. 1999.

[3] A. Glière, J. Rouxel, B. Parvitte, S. Boutami, and V. Zéninari, "A Coupled Model for the Simulation of Miniaturized and Integrated photoacoustic Gas Detector," *Int. J. Thermophys.*, vol. 34, no. 11, pp. 2119–2135, Nov. 2013.

[4] Rouxel, J., Coutard, J.-G., Gidon, S., Lartigue, O., Nicoletti, S., Parvitte, B., Vallon, R., Zéninari, V., Glière, A., Development of a miniaturized differential photoacoustic gas sensor, Procedia Engineering, 120, 2015,

03

SILICON PHOTONICS

- CMOS photonics III-V /Si devices
- Modulators and receivers
- Hybrid optical lasers
- Photonic systems

Progresses in 300mm DUV photolithography for the development of advanced silicon photonic devices

Research topic: silicon photonics; patterning

C Baudot*, B Szelag, N Allouti, C Comboroure, S Bérard-Bergery, C Vizioz, S Barnola, F Gays, D Mariolle, T Ferrotti, A Souhaité, S Brision, C Kopp, S Menezo
(* STMicroelectronics, Crolles, France)

Abstract: we report on advances in DUV dry photolithography both for etching and implantation of silicon photonic devices. We explain why silicon patterning is a critical building block in silicon photonics and what are the challenges related to that process. Furthermore, it also occurs that some silicon photonic devices need implantation lithographic conditions which are also specific to the technology. For that purpose, we developed a dedicated DUV 193nm implantation lithography to address that need.

Main Results

Simulations using Eigen Mode Solver of Lumerical Mode Solution have been performed to understand better the challenges of waveguide design. The first consideration is to properly determine the rib waveguide cross-section and the bends configuration. First, the influence of silicon etch profile variation on Insertion Losses (IL) has been estimated. The roughness simulations were performed using Lumerical FDTD 3D Solutions. The pertinence of the model with respect to actual devices has been evaluated from a morphological point of view. A SEM analysis of strip (Fig. 1b) and rib (Fig.1c & d) waveguides shows, indeed, that defects have a vertical symmetry probably issuing from a roughness transfer between the photoresist and silicon during etching. Fig. 1e shows the IL simulated results with respect to the defect size. Losses are negligible for very small roughness but they rapidly increase quasi-exponentially for bigger anomalies. Consequently, we conclude that lateral sidewall roughness plays a predominant role in patterning process for silicon photonics.

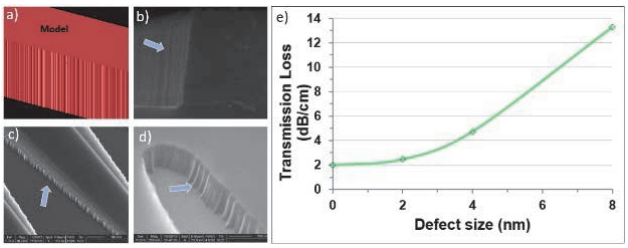

Figure 1. 3D view of the scripted rough waveguide. b) SEM observation of a strip waveguide showing strong correlation with the model. c) & d) same observations for a rib waveguide. e) Simulated IL with respect to the defect size.

There are a few factors that must be taken into account during silicon patterning. During the photolithography processes some features that are specific to silicon photonics must be considered. The targeted structures vary a lot within the same design in many aspects.

The Echelle grating is a perfect example to illustrate the singularities of silicon photonics (Fig. 2). The working principle of the device consists of diffracting a signal issued from a waveguide with the use of a reflective grating so that the diffracted image converges towards another waveguides.

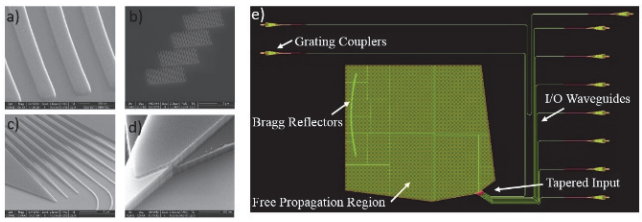

Figure 2. Various components present in an Echelle grating: a) The fiber grating coupler. b) The arrays of Bragg reflectors. c) Tapering region between strip and rib waveguides. d) Closer view of the transition zone. e) Overview of the whole device.

To reach all these different small CD (Critical Dimension) values, a lot of attention is paid during the lithography step. More precisely, the different proximity effects are taken into account while considering such dimensions. These resolution enhancement topics are mainly addressed through the use of Optical Proximity Corrections (OPC) on the layout before the mask manufacturing.

There is another specific photolithography development which has been performed for silicon photonics. It is an implantation lithography which is intended for Mach-Zehnder modulators .More particularly, it addresses the particular needs of PIPIN and interleaved modulators. The challenges of that lithography are, first, the ability to make isolated trenches of 120nm and, secondly, to make array trenches of 200nm pitch and a duty cycle of 0.5. To realize such an aggressive implantation lithography, 193nm dry lithography is necessary. Moreover, to achieve the targeted CD, the photoresist thickness cannot be too big because of aspect ratio issues.

Perspectives

The challenges of future silicon photonic technology nodes can be achieved by amending some process building blocks. Even if the first technology nodes have been fabricated using essentially standard CMOS processes with minor customizations, we observe that future demands in silicon photonics will require more aggressive and targeted processes. We show why silicon patterning is the building block where the biggest challenges may come from.

Related Publications:
[1] Chabloz, M., Sakai, Y., Matsuura, T., Tsutsumi, K., “Improvement of sidewall roughness in deep silicon etching,” Microsyst. Technol., (2000)
[2] Marris-Morini, D., Baudot, C., Rasigade, G., Fedeli, J.M., Vulliet, N., Souhaite, A., Ziebell, M., Crozat, P., Bouville, D., Menezo, S., Boeuf, F., Vivien, L., "High speed silicon modulators on 300 mm SOI wafers," 10th IEEE GFP, 87-88 (2013).
[3] Marris-Morini, D., Baudot, C., Fédéli, J.M., Rasigade, G., Vulliet, N., Souhaité, A., Ziebell, M., Rivallin, P., Olivier, S., Crozat, P., Le Roux, X., Bouville, D., Menezo, S., Bœuf, F., Vivien, L., “Low loss 40 Gbit/s silicon modulator based on interleaved junctions and fabricated on 300 mm SOI wafers,” Opt. Express 21(19), 22471-22475 (2013)
[4] Baudot, C., Szelag, B., Allouti, N., Comboroure, C., Bérard-Bergery, S., Vizioz, C., Barnola, S., Gays, F., Mariolle, D., Ferrotti, T., Souhaité, A., Brision, S., Kopp, C., Menezo, S., Progresses in 300mm DUV Photolithography for the Development of Advanced Silicon Photonic Devices, Proceeding SPIE, 94260D, 2015.

Records of amplified strain on 200 mm optical Germanium-On-Insulator (GeOI) substrates: a step towards CMOS compatible Ge lasers

Research topic: Germanium on Insulator, Tensile strain, laser, Band structures engineering

V Reboud, V Calvo*, J Widiez, J.M Hartmann, A Gassenq*, STardif*, K Guilloy*, N Pauc*, J. Rothman, F Rieutord*, I Duchemin*, Y. M. Niquet*, A Gliere, A Chelnokov (* CEA, INAC, Grenoble, France)

Abstract: One of the main challenges in the field of silicon photonics is currently the fabrication of efficient laser sources compatible with the microelectronic fabrication technology. Ultra-high strains can theoretically transform the Germanium from an indirect to a direct bandgap semiconductor. We showed that the high crystalline quality of GeOI layers fabricated by Smart Cut™ technology dramatically improved the mechanical failure limits when liberating the Ge microbridges. Record strain level of 1.9% for biaxial and 4.9% for uniaxial stress were reached by carefully designing the geometry of micro-structures. A new strain-Raman shift relation was demonstrated using synchrotron Laue micro-diffraction at ESRF.

Context and Challenges

The indirect bandgap of group IV (Ge or Si) elements prevents them from being used as efficient light-emitters. Different approaches have been proposed to over-come the indirect bandgap of Ge, such as doping, strain adding, or Sn alloying. Germanium under high mechanical strain is indeed with GeSn alloy a promising materials to be used as light emitter for the monolithic integration of photonic circuits on silicon-based electronics. Main challenges are (i) to reach unprecedented strain values predicted theoretically to transform Ge into a direct band-gap materials and (ii) to get access to accurate high strain micro-measurements in Ge.

Main Results

To reach such challenging high level of strains predicted for an indirect-direct transition [1], we used high quality optical GeOI substrates with a low density of threading dislocations. We showed that the thick Ge withstands high-strains redistribution in Ge micro-bridges, while providing optical confinement and low propagation losses of the optical modes [2].

To redistribute and amplify the residual tensile strain present in optical GeOI substrates, membranes were fabricated using sets of design rules. Tensile strain was first quantified using micro-Raman spectroscopy with an input laser at 785 nm wavelength focused in the center of the microbridges (giving a light penetration depth of 220nm).

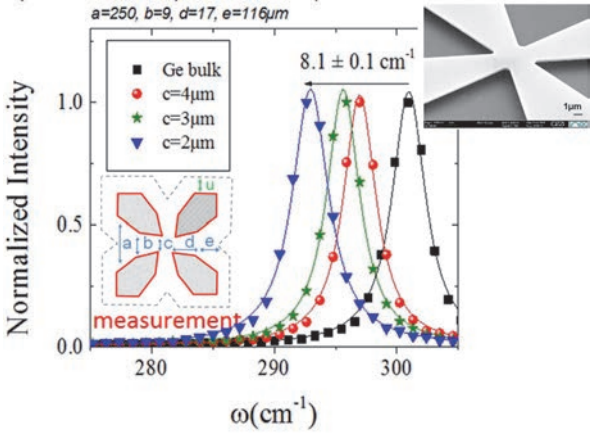

Figure 1: Raman spectroscopy measurement for a Ge bulk substrate and for different Ge biaxial membranes measured in the center of the microbridges. Titled SEM image of a studied biaxial Ge membrane.

When reducing the central dimension of the micro-bridge (Figure 1), the measured tensile strain increases from 1.1% up to 1.4% and finally a record breaking 1.9% [3].

Tensile strains were accurately measured in Ge using X-ray Laue and rainbow-filtered Laue micro-diffraction at beam-line BM32 of the European Synchrotron Radiation Facility. Figure 2 presents the measured strain as function of the spectral Raman shift. Our direct measurement of strain allow us to calibrate for the first time the strain-to-Raman-shift up to uniaxial tensile strain of an unprecedented level of 4.9 %.

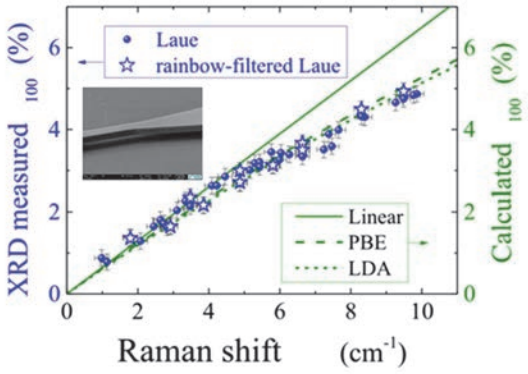

Figure 2: Raman strain relation: measured strain by micro-XRD (dots), simulated strain by ab initio calculations (dotted lines), and linear empirical dependence (solid line). Titled SEM image of a studied uniaxial Ge membrane.

For uniaxial stress along <100> in Ge, the common linear empirical relation was widely used in the literature to link Raman shift to strain in Ge. The following equation provide the revisited strain-shift relation over the 0-5 % tensile strain and 0-10 cm^{-1} shift range [4], where Δω is the Raman shift value.

$$\varepsilon_{100} = 0.68(\pm 0.02)\ \Delta\omega - 0.021(\pm 0.002)\ \Delta\omega^2$$

For biaxial strain, strain-shift relation was verified to be linear following this equation:

$$\varepsilon_{100} = 0.237(\pm 0.02)\ \Delta\omega.$$

Perspectives

Building on the high crystalline quality of GeOI substrates, we demonstrate uni-axial tensile strain of 4.9% and bi-axial tensile strain of 1.9%, which is currently the highest reported value measured in thick (350 nm) Ge layer. Since such strains are generally considered as the onset of the direct bandgap in Ge, our realization paves the way towards mid-infrared lasers fully compatible with CMOS fabrication technology.

Related Publications:
[1] J. M. Escalante, *et al*., Non-linear model of electronic band structure to highly tensile-strained Germanium, Proc IEEE, 7305955-77(2015).
[2] V. Reboud, *et al*., Structural and optical properties of 200 mm germanium-on-insulator (GeOI) substrates for silicon photonics applications Proc. SPIE 9367, 936714 (2015)
[3] A. Gassenq, *et al*. 1.9% bi-axial tensile strain in thick germanium suspended membranes fabricated in optical germanium-on-insulator substrates for laser applications Applied Physics Letters 107, 191904 (2015)
[4] A. Gassenq, *et al*. Accurate strain measurement in highly strained Ge microbridges, submitted.

Up to 20 Gb/s directly-modulated hybrid III-V on Si lasers in the C-band for access networks

Research topic: Silicon Photonics, III-V on Si hybrid lasers, direct modulation, access networks

S. Olivier, S. Malhouitre, C. Jany, C. Kopp, G.H. Duan*, A. Accard*, P. Kaspar*, G. de Valicourt*, G. Levaufre*, N. Girard*, A. Leliepvre*, A. Shen*, D. Make*, F. Lelarge*, F. Mallecot*, P. Charbonnier*, H. Garriah*, J.-L. Gentner* (*III-V Lab , Palaiseau, France)

Abstract: Silicon photonics is a very attractive platform for the development of compact, low-cost and energy-efficient photonic circuits, co-integrated with their electronic circuits. The integration of the laser source is key to reduce packaging costs and allow for large scalability. We have used the molecular bonding technique to develop hybrid III-V on Silicon lasers. After the development of hybrid III-V on Silicon tunable lasers with excellent performances in terms of tunability and single mode behavior, we demonstrate direct modulation at 10 and 20 Gb/s using such lasers. High data rate modulation is obtained by engineering a second resonance in the electro-optic modulation response of the laser.

Context and Challenges

Silicon photonics is attracting a lot of attention due to the prospect of compact, low-cost and energy-efficient circuits that integrate photonic and microelectronic elements on a single chip. Silicon photonics is suited for a wide range of applications from long-haul transmission to short-distance data communications.

However the laser is the key component missing in this technology. In the absence of practically efficient lasers directly achievable in Silicon or Germanium today, hybrid integration of III-V material on Silicon by molecular bonding seems to be a very promising solution. This approach exploits the highly efficient light emission of direct band gap III-V material and the compact and low-loss photonic circuitry in silicon. In contrast with flip-chip or butt-coupling techniques, no critical alignment between the III-V material and the SOI wafer is required.

We have developed a continuous-wave hybrid III-V on Si widely tunable laser with excellent performances in terms of threshold current, monomode behavior, output power and tunability in the last years, suitable for to meet metropolitan network specifications.

Direct modulation of such tunable lasers at 2.5 and 10 Gb/s is highly desirable for low-cost next generation optical network units (ONU) in access networks. The requested reach is expected to be at least 40 km. The absence of external modulators could significantly reduce the power consumption while the tunability will provide the wavelength flexibility required for this type of network.

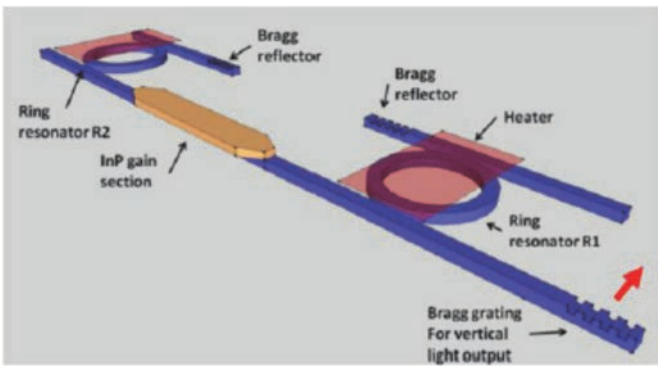

Fig. 1: Architecture of a hybrid III-V on Silicon tunable laser with a double ring resonator filter integrated in the laser cavity.

Main Results

The architecture of our tunable laser is sketched in Figure 1. It consists of an InP-based amplification section, tapers for modal transfer between III-V and Si waveguides, two slightly different silicon ring resonators taking advantage of the Vernier effect for single mode selection, metal heaters on top of the ring resonators for thermal tuning and silicon Bragg gratings providing reflection and output fiber coupling. The fabricated tunable lasers are packaged in a butterfly optical module, achieving a wavelength tuning range of 35 nm, a side mode suppression ratio of 50 dB and an optical power coupled to a monomode fiber in excess of 4 mW across the whole wavelength range.

Such tunable laser is then tested for direct modulation. The laser is biased at 82 mA in CW and a 3 Vpp random non-return-to-zero (NRZ) random bit sequence at 10 Gb/s is applied through a high-frequency bias tee. The optical power coupled into the monomode fiber was -8.7 dBm, using non-optimized fiber grating couplers.

BER results of transmission distances from 0 to 60 km are presented in Figure 2, either with or without pre-emphasis of the electrical signal. The received power after 40 km transmission with pre-emphasis at the 3.8 10^{-3} BER limit (compatible with hard decision forward error corrector HD-FEC) was measured to be -26.5 dBm, corresponding to an optical power budget of 18 dB. The power penalty is only -0.5 dB with respect to back-to-back transmission. These results illustrate the capability of hybrid tunable lasers to reach a significant distance without any regeneration or chirp filtering.

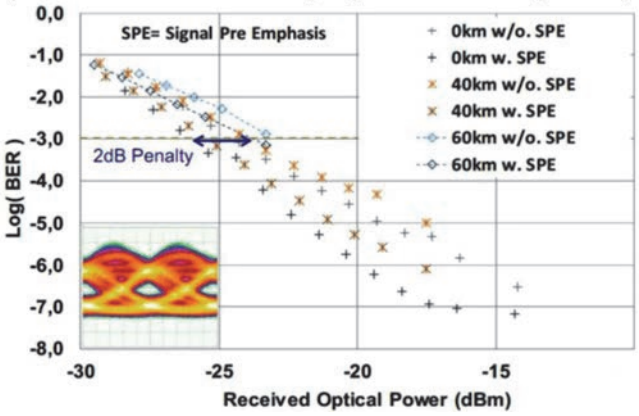

Fig. 2: BER measurements at 10 Gb/s with back-to-back eye diagram (inset)

In order to increase the data rate beyond 10 GB/s, the electro-optic modulation bandwidth has to be increased. By adjusting the laser cavity passive length of 1 mm by heating one ring resonator, the spacing between the main laser mode and a second mode, spectrally close to the main one, can be adjusted. The beating of these two modes is at the origin of a second resonance frequency, clearly visible in the electro-optical modulation response. shown in Figure 3, leading to an enhancement of the modulation bandwidth.

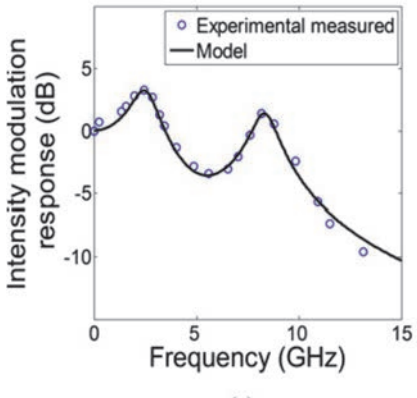

Fig. 3: Electro-optical response of the hybrid III-V on SOI tunable laser at I=110 mA

The hybdrid laser is directly modulated using a 20 Gb/s random bit sequence. The ouput power coupled into the monomode fiber is – 8 dBm (again with non-optimized fiber grating couplers). The BER measurement in back-to-back configuration is shown in Figure 4 for 12 different wavelengths in the C-band, selected within the tunable range of the laser. For all those wavelengths, the BER can reach the 3.8 10^{-3} BER limit (compatible with hard decision forward error corrector HD-FEC).

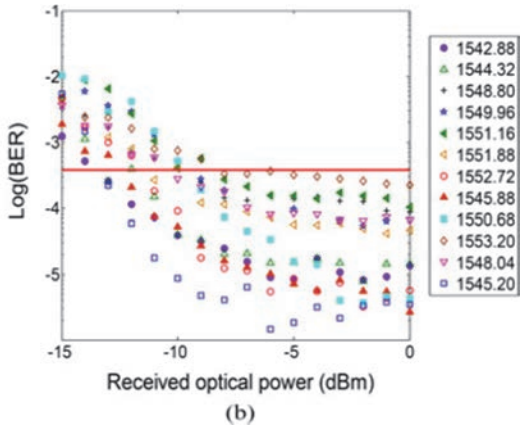

Fig. 4 : BER measurement at 21 Gb/s depending on the received optical power for various wavelengths in back-to-back configuration

Perspectives

These results illustrate that III-V hybrid tunable lasers, initially developed for CW operation in metropolitan networks, can also be directly modulated for access network applications. Transmission over 60 km was demonstrated at 10 Gb/s and 20 Gb/s operation was demonstrated in back-to-back configuration without any chirp filtering.

Such high data rate is achieved thanks to the engineering of a second resonance in the electro-optic response of the laser. The chromatic dispersion is also drastically reduced thanks to the integrated narrow filter formed by the double ring resonator configuration. In addition, this double ring resonator filter allows to tune the laser wavelength in a very short time (> 1ms) over a wide range of 35 nm, thus providing a flexible and efficient transmitter in the C-band.
The power budget could be further improved by increasing the output power of the laser to 5 dBm, thus allowing to meet Next Generation specifications of Passive Optical Units (NG-PON2) in access networks.

Related Publications:
[1] "Hybrid wavelength-tunable III-V lasers on silicon", G.-H. Duan, C. Jany, A. Leliepvre, A. Accard, P. Kaspar, A. Shen, P. Charbonnier, F. Mallecot, F. Lelarge, J.-L. Gentner, S. Olivier, S. Malhouitre and C. Kopp, SPIE Newsroom 10.1117/2.1201403.005370 (2014)
[2] "New advances on heterogeneous integration of III-V on Silicon", G.-H. Duan, S. Olivier, S. Malhouitre, A. Accard, P. Kaspar, G. de Valicourt, G. Levaufre, N. Girard, A. Leliepvre, A. Shen, D. Make, F. Lelarge, C. Jany, K. Ribaud, F. Mallecot, P. Charbonnier, H. Garriah, C. Kopp and J.-L. Gentner, J. of Lightwave Technol., 33, 976 (2015)

Silicon Photonics Modules: from circuit design to system level test

Research topic: silicon photonics, Photonic Integrated Circuit, optoelectronic module, packaging

S Bernabé, B Blampey, O Castany, B Charbonnier, A Myko, M Fournier, B Szelag, S Menezo and C Kopp

Abstract: Based on mature silicon photonic devices like high speed photodiodes, low loss waveguides, wavelength filters and modulators, complex Photonic Integrated Circuits can be built in order to address various optical fiber transmission applications. Packaged demonstrators using Photonic Integrated Circuits have been designed and tested for three classes of optical networks: telecommunication networks, access networks and datacom networks.

Context and Challenges

In the past years, Silicon Photonics technology has reached a level of maturity that enables the development of Photonic Integrated Circuits (PICs) of increasing complexity, to address various fields of applications, for example long haul telecommunication using advanced modulation formats (like QPSK), access networks (e.g. Fiber To The Home) and short reach datacom transmissions at 25Gbps per channel in data centers. Each application has specific requirements and challenges in terms of module integration, packaging and system level test.

Main Results

In the frame of various collaborative projects (ANR ULTIMATE and FAON, EU FP7 FABULOUS, ANR IRT Nanoelec, EU FP7 PLAT4M), we have developed a wide range of PICs addressing the three applications mentioned above [1]. The circuits have been processed at LETI, on 200mm wafer, using 220/2000nm or 310/800 nm Silicon-On-Insulator (SOI) substrates (Figure1).

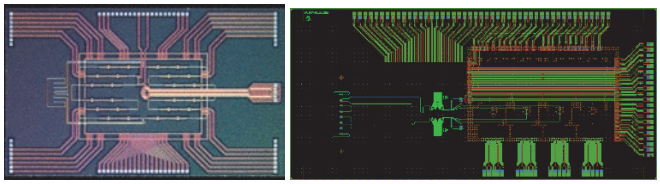

Figure 1 - Example of Photonic Integrated Circuits: Reflective Modulator for Access Networks (FABULOUS project) (left), 4 channels Photoreceiver circuit layout (PLAT4M project). Both circuits are designed to be operated by flip-chipped driving electronics from ST Microelectronics.

PIC design notably includes a particular attention to be paid on the RF electrodes design. For this, electromagnetic simulations are used to ensure the required signal integrity to be guaranteed from the driving device (transimpedance amplifier or modulator driver) to the photonic active device (photodiode or modulator, respectively)[2]. To achieve module integration of these PICs, optical fiber arrays have to be accurately aligned and attached to the chip (Figure 2). This operation is performed by using active alignment processes on dedicated equipment (like Nanosystec Nanoglue).

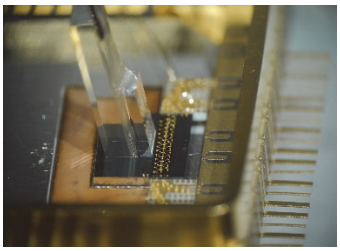

Figure 2 – Detail view of a packaged Reflective Modulator (ANR FAON project), using a metallic OIF package and a pigtailed fiber array.

Final step of module integration is the module test itself, in a system environment. In the frame of the projects mentioned above, we have performed transmission tests on telecommunication transmitter modules (BPSK transmission at 25 Gbps)[3], transmitter module for FTTH (based on Reflective Modulator) [4], and multichannel 4x25Gbps photoreceiver for data center communications (Figure 3).

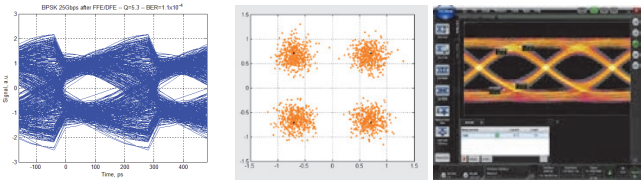

Figure 3 – Three examples of system level test results: (a) 25 Gbps eye diagram at the output of a BPSK modulator (ANR ULTIMATE), (b) QAM-4 constellation at the output of a Reflective Modulator (FP7 FABULOUS), (c) 25 Gbps eye diagram at the output of one channel of a 4x25Gbps photoreceiver (IRT Nanoelec)

Perspectives

Our capacity to build system-level demonstrators using our Photonic Integrated Circuits and related packaging technologies will be applied to new generation of devices requiring high level of complexity, like Terabit class transceivers, scalable integrated switch matrices and optical Network On Chips.

Related Publications:
[1] O. Castany, C. Kopp, S. Bernabe, and J. M. Fédéli, “Advances in silicon photonics integration with electronics to move more data faster,” in Opto-Electronics and Communications Conference (OECC), 2015, 2015, pp. 1–1.
[2] B. Blampey, S. Bernabé, K. Rida, O. Castany, A. Myko, C. Kopp , “Challenges for Silicon Photonics Based Mid Board Modules to Achieve High Data Rate Transmissions” in Progress in Electromagnetics Research Symposium (PIERS) , Prague, 2015 (invited, abstract online)
[3] S. Bernabé, et al., “High-Speed Coherent Silicon Modulator Module using Photodiode Integrated Circuits: from Circuit Design to packaged module” in Proceedings of SPIE, 9891,35, Photonics Europe, Brussels, 2016 .
[4] S. Menezo et al., “Transmitter Made up of a Silicon Photonic IC and its Flip-Chipped CMOS IC Driver Targeting Implementation in FDMA-PON,” Journal of Lightwave Technology, vol. 34, no. 10, pp. 2391–2397, May 2016.

04

SOLID STATE LIGHTING (LED)

- Microwires & Nanowires light emitters
- Growth of high quality GaN on Si
- GaNoS advanced substrates
- Strain distribution in GaN
- Efficiency of LED phosphors
- LED packaging

High quality GaN material grown on textured N-polar AlN on Si (100) for µ-LED application

Research topic: GaN, silicon, selective area growth

G. Laval, A. Dussaigne, G. Feuillet, P. Ferret, N. Mante, S. David*, T. Baron*
(*CNRS/UJF/LTM, Grenoble, France)

Abstract: In order to grow high crystalline quality GaN on silicon substrate, complex processes are currently necessary. To avoid using these time-consuming techniques, selective area growth of N-polar GaN micron-sized platforms is investigated. Growth is performed on a textured AlN layer to prevent Si melt-back etching, thus allowing epitaxy on Si (100). Using a two steps process, fast strain relaxation is evidenced while platforms' surface displays a reduced dislocation density (estimated average value: 6.10^8 cm^{-2}), highlighting the efficiency of our simple process. These results indicate that platforms' top GaN material is suitable as pseudo-substrate for micro light emitting (µ-LEDs) diodes epitaxy.

Context and Challenges

For several years, more and more attention is given to silicon as substrate for GaN optoelectronic devices due to its low cost and availability in large diameter. It also makes devices' integration to microelectronics and packaging easier. However, growing good quality material on Si remains a challenge. Indeed, current time-consuming solutions require several layers to reduce dislocation density and to prevent crack formation [1-3]. We propose to grow by metalorganic vapor phase epitaxy GaN platforms suitable as pseudo-substrates for µ-LEDs epitaxy thanks to selective area growth (SAG).

Main Results

Silicon substrate was protected from melt-back etching [4] by a layer of N-polar AlN. Indeed, on a wide range of conditions, SAG N-polar GaN structures present a flat top with vertical sidewalls (unlike Ga-polar material which present a pyramidal morphology) [5]. As there are still issues to grow monocrystalline N-polar AlN on Si, a physically vapor deposited textured layer has been used, allowing loss of connection with the substrate, thus enabling growth on Si(100). Two steps growth process then took place through a SiN mask (2 µm-diameter holes, 10 µm pitch): firstly, small platform growth to relax tensile strain and start bending dislocations; afterwards, broadening step to get flat material presenting an improved crystalline quality top surface.

SEM image of non-broadened platforms (not shown here) reveals a multigrain aspect, owing to the presence of several AlN grains in each mask opening. However, under optimized broadening conditions, seemingly monocrystalline hexagonal flat GaN platforms have been obtained presenting a homogenized morphology, as displayed in Fig. 1a.

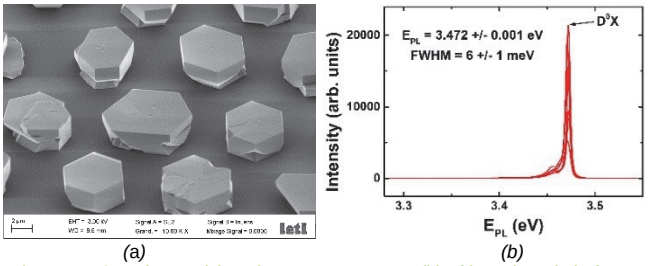

(a) (b)

Figure 1 – SEM image (a) and µPL spectra at 4K (b) of broadened platforms

Micro-photoluminescence (µPL) characterizations have been performed. As shown in Fig.1b, donor bound exciton of GaN near band edge (NBE) is observed at 3.47 eV, revealing a relaxed tensile strain directly after first growth step [6]. Moreover, thanks to enlargement step, NBE linewidth has been reduced from 32 to 6 meV, demonstrating a high crystalline quality material despite both the textured nucleation layer and the growth on Si(100).

TEM characterizations (displayed in Fig. 2) revealed that while some dislocations propagate to platform's surface, others bend in broadened regions. Presence of several grains in platforms also turned out to help improving quality by blocking dislocations at grain boundaries. Estimated dislocation density measured by cathodoluminescence revealed an average value of 6.10^8 cm^{-2}, thus displaying the efficiency of our simple growth process. CL and TEM characterizations are currently being paired to observe dislocations' behavior in platforms and their effect [7].

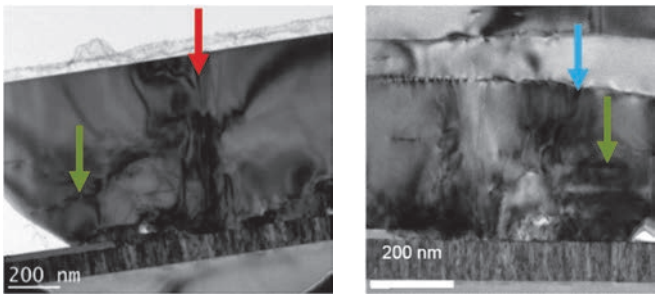

Figure 2 – TEM images showing threading dislocations (red arrow), bent dislocations (green arrows) and blocked dislocations at grain boundaries (blue arrow)

Perspectives

All these results indicate that these platforms present a top GaN material suitable as pseudo-substrates for µ-LED epitaxy. Growth attempts of InGaN/GaN quantum wells growth on their top are currently being performed. N polarity should enable better indium incorporation than on Ga-polar surface, giving the chance to realize long wavelength emission µ-LEDs.

Related Publications:
[1] A. Watanabe et al, J. Cryst. Growth, vol. 128, pp. 391–396, 1993,
[2] E. Feltin et al, Phys. Status Solidi, vol. 535, no. 2, pp. 531–535, 2001,
[3] F. Semond et al, Appl. Phys. Lett., vol. 78, no. 3, p. 335, 2001,
[4] H. Ishikawa et al, J. Cryst. Growth, vol. 189–190, pp. 178–182, 1998,
[5] X. J. Chen et al, Appl. Phys. Lett., vol. 97, no. 15, pp. 2008–2011, 2010,
[6] K. Naniwae et al, J. Cryst. Growth, vol. 99, pp. 381–384, 1990.
[7] G Laval et Al, Inter. Conference on Nitride Semiconductors (ICNS 2015)

III-N MOVPE overgrowth, material quality and LED structures on GaNoS and GaNoMo advanced substrates

Research topic: GaN, MOVPE, GaNoS, substrates

A. Dussaigne, P. Ferret, R. Obrecht, M. Lafossas, A. Coquiard, A. Fargeix, R. Caulmiloné*, P. Guénard* and F. Lévy (*SOITEC, Bernin, France)

Abstract: High material quality of GaN overgrown by MOVPE is demonstrated on thin Ga-polar GaN seed layer transferred on sapphire (GaNoS) and on molybdenum (GaNoMo) substrates thanks to a SiO_2 bonding layer. GaN material quality of the original GaN template can be recovered after 1µm thick GaN overgrowth. LED structures are also compared on these particular substrates together with same structure on GaN template on sapphire.

Context and Challenges

In the past years, SOITEC company developed an original process to transfer a thin GaN layer from a donor GaN template to another substrate (sapphire, silicon, …) [1]. This process is based on the Smart Cut ™ technology, combining ion implantation for splitting and oxide direct bonding for the transfer, and allows the re-use of the initial donor template several times. These substrates could be available in large size if original donor GaN templates with same size substrate could be provided. This transferred GaN layer is highly resistive due to the use of an ion implantation technique and can be an interesting candidate as a new substrate for power electronics. GaN could also be available on either Ga-polar or N-polar side. Using this process, one can imagine a transfer of GaN on a substrate suitable for GaN MOVPE overgrowth on large size substrates. This is the purpose of the GaN on molybdenum approach [2]. Indeed, the main interest is to obtain a substrate with closer value of thermal expansion coefficient as GaN, compared to standard sapphire substrate. In this case, for such Mo substrates (4", 6", 8"), bow should not vary during cooling down after GaN based device overgrowth.

Main Results

First, up to 5 µm thick GaN overgrowth has been performed by MOVPE on GaNoS substrate. No delamination or cracks have been observed, showing the high strength of the oxide-oxide bonding above 1000°C. With only 150 nm of transferred GaN, it is possible to recover GaN template quality on a 1µm thick overgrown layer both in terms of structural and optical quality. Indeed, omega scan linewidth as low as 237 arcsec and near band edge linewidth (D°X) as low as 3.5 meV have been measured. Then, LED structures have also been grown on both GaNoS and GaNoMo substrates. A basic heterostructure has been chosen for a first test: after 1 µm of GaN overgrowth, 2.5 µm of n-type GaN has been grown followed by 5 InGaN/GaN multiple quantum wells (MQWs), 20 nm of p type AlGaN and 220 nm of p type GaN. X-ray diffraction measurements have been carried out on these two LED epiwafers. Fig. 1 presents (002) omega scans. In case of GaNoS, linewidth is 254 arcsec and is close to original GaN template. A slightly larger linewidth is observed on GaNoMo. Not enough data are available yet to conclude if it is due to Mo substrate, but in any case the value (300 arcsec) is low enough to say that structural GaN quality is good on GaNoMo [3].

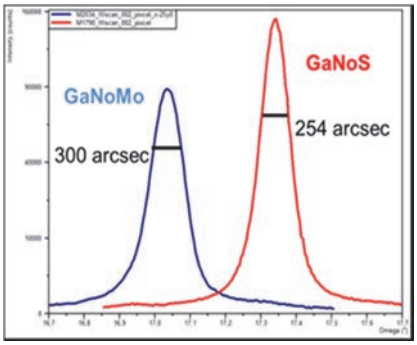

Fig.1: X-Ray scans of full LED structures grown on Ga-polar GaNoMo and GaNoS by omega scan (002)

Then, LED structures on GaNoS, GaNoMo and template have been processed: half of the 4 inch wafer with reflective p-electrode (reference process), half with semi-transparent p-electrode in order to compare with GaNoMo. As displayed by Fig.2(a), in case of reflective p-electrode, EQE value of 9% is obtained at 35 A/cm² which is a good value knowing that nothing has been done to favor light extraction.

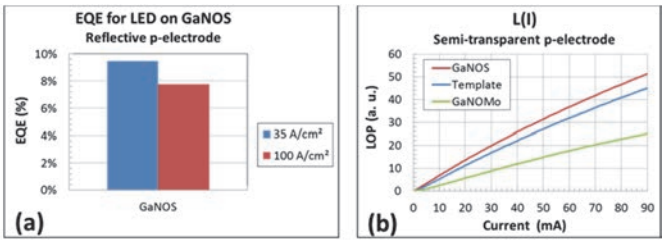

Fig.2: (a) EQE for LED on GaNoS in case of reflective p-electrode. (b) Light Output Power (LOP) as function of current for LED on GaNoS, GaNoMo and template in case of semi-transparent p-electrode.

Finally, for semi-transparent p-electrode (Fig.2(b)), GaNoS and template LOP values are very close. It is only divided by 2 in case of GaNoMo, demonstrating for the first time the possibility to grow LED on Mo substrate.

Perspectives

More work has now to be done both on GaN transfer on Mo substrate and on Mo substrate itself in order to demonstrate the effective flatness of GaN based structure on large size Mo substrate.

Related Publications:
[1] A. Tauzin *et al.*, "Transfer of two inch GaN film by the Smart Cut™ technology", ECS proceedings 06, 119 (2005)
[2] M. Seiss *et al.*, to be published
[3] A. Dussaigne, P. Ferret, R. Obrecht, M. Lafossas, A. Coquiard, A. Fargeix, R. Caulmiloné, P. Guénard and F. Lévy, III-N MOVPE overgrowth, material quality and LED structures on GaNoS and GaNoMo advanced substrates, Proceeding Inter. Conference on Nitride Semiconductors (ICNS 2015)

Strain distribution in GaN epilayers on Si-based substrates

Research topic: GaN, strain, dislocations, TEM, N-PED

N. Mante, G. Feuillet, N. Bernier, V. Delaye, J-L. Rouvière*, P. Vennéguès**
(*CEA/ DSM_INAC, ** CNRS/CRHEA - Sophia Antipolis - France)

Abstract: When grown on Silicon substrates, GaN epilayers are subject to stresses arising from the lattice and thermal mismatches with the substrates. We have compared the strains in GaN epilayers grown either on silicon or on SOI substrates. In the last case, the idea was to demonstrate compliance effects. Complementary TEM techniques were used to assess the strains: diffraction contrast, HR(S)TEM, and nanobeam electron diffraction in precession mode (N-PED). In the case of SOI substrates, the presence of residual strains in the top silicon layer was attributed to partial stress transfer from epilayers to substrate. Strain maps and profiles yield complementary information about the stress evolution within the nitride layers during and after growth, closely related to the behavior of dislocations.

Context and Challenges

This work deals with the precise measurement of strain in nitride epilayers grown on Silicon and Silicon-on-Insulator (SOI), using advanced TEM techniques. In order to cope with growth issues when using Si as a substrate for nitrides, strain engineering is necessary. This is usually carried out through the insertion of strain compensating layers before the growth of the active regions, which adds up to the growth duration and complexity. An alternative method consists in using compliant substrates, possibly SOI, for potentially accommodating strain during growth and/or upon cooling down.

Main Results

We investigated the influence of the mismatch on a possible compliance effect. For this purpose, the nitride layers were grown onto <110> oriented silicon. A c-oriented AlN buffer layer is grown first before the proper c-oriented GaN layer.
For this particular c-AlN / <110>-Si interface, the mismatch is large in one direction (18% for <10-10>-AlN // <001>-Si) and low in the perpendicular direction (below 1% for <11-20>-AlN // <-110>-Si) [1].
A first evaluation of strains occurring during growth can be undertaken by counting misfit dislocations (MD) at the hetero-interface. Here the number of MD at the AlN/Si interface was compared for the two perpendicular directions. More specifically this was carried out for two samples: GaN/AlN/Si <110> and GaN/AlN/SOI whose top silicon is <110>-oriented and only 16 nm thick. For both samples, in the large mismatch <10-10> interface direction, a MD was found every 5 AlN planes suggesting complete relaxation in this direction. For the perpendicular interface direction we found 1 MD every 125 AlN planes for bulk Si bulk substrate, while only 1 every 258 AlN planes in the case of the SOI substrate. This indicates a slight tensile stress in the case of AlN on SOI substrate.
In order to assess any elastic compliance effect, the strain distribution was measured in the nitride layers and the top silicon layer of the SOI. TEM measurements were carried out in a FEI Titan3 Microscope using Nano beam electron diffraction (NBED) in precession mode [2]. This technique combines high spatial resolution (2 nm), good strain precision (2×10-4) and large area analysis (a few µm²). In the low mismatch AlN / Si interface direction, the measurements in figure 1 show clearly some compressive strain in the top silicon layer of the SOI, which is not the case when dealing with the AlN / bulk Si interface, for which no strain was measured in the silicon. Our explanation is that some stress has been shared between the AlN layer and the top silicon layer [3].

The measurement of lattice rotations within the layers is displayed on figure 1-b and reveals undulations in the top Si layer, also attributable to strain relaxation.

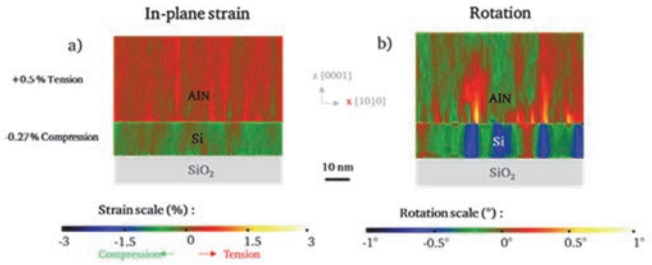

Fig 1: a) In-plane strain and b) rotation at the AlN/SOI interface, for the low mismatch direction.

Moreover, the in-plane strain profile was determined by N-PED in GaN and AlN as plotted in figure 2. We note the strain inversion at a certain thickness in the GaN layer: from compression next to the AlN interface to tension further up in the layer. Compression at the early stage could be attributed to the 2.5% lattice mismatch strain between GaN and AlN gradually relaxed through the formation of dislocation loops, while the residual tensile strain is related to the remaining bent dislocations in the upper part of the layer.

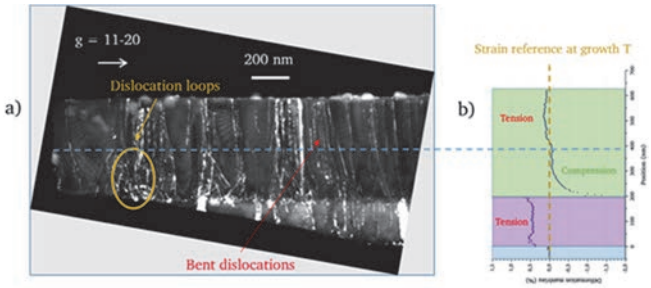

Fig 2: a) Weak-beam images of dislocations in a GaN/AlN/Si sample compared to b) in-plane strain profile at growth temperature.

Perspectives

We were able to demonstrate the presence of residual in-plane strain and rotation in the top silicon layer of an SOI substrate, attributable to partial stress transfer from the AlN layer to the substrate, but only in the case of thin silicon and for the low interface mismatch direction. We found a strong relationship between the behavior of dislocations as growth proceeds and the shape of the strain profile.

Related Publications:
[1] Cordier Y. et al, "Growth of GaN based structures on Si (110) by molecular beam epitaxy", Journal of Crystal Growth, Vol. 312, pp 2683-2688, 2010.
[2] Rouvière J-L. et al, "Improved strain precision with high spatial resolution using nanobeam precession electron diffraction", Applied Physics Letters, Vol. 103, pp 241913, 2013.
[3] Mante N., Feuillet G., Bernier N., Delaye V, Strain Study of GaN on Si-Based Substrates, Proceeding Inter. Conference on Nitride Semiconductors (ICNS 2015)

A wafer level approach for LED packaging using “TSV-last” technology

Research topic: Wafer level packaging, TSV, LED

M. Volpert, B. Soulier, S. Borel, N. Ait-Mani, S. Gaugiran, A. Gasse, D. Henry

Abstract: An innovative wafer level packaging approach is presented here for the packaging of nanowires LED. In this approach the GaN LEDs are first fabricated by the epitaxial growth of GaN nanowires on Silicon substrate, then the chip color conversion and mechanical protection is achieved at the wafer level as well as the connecting pads and redistribution layer. These technologies are achieved using Through Silicon Vias (TSV) with high aspect ratio.

Context and Challenges

If the high efficiency of the LED technique is proven, lots of work remains in the packaging field for cheaper and more reliable systems. Indeed up to 60 % of the overall LED production cost falls on the packaging as most of the LED packaging is achieved on individual chips [1]. The most widely spread packaging configuration deals with wire bonding electrical contact as opposed to bump bonding. In this case the package footprint is not optimum, and it demands an additional wire bonding step. Ideally after being fabricated the LED should be directly available as a SMT (surface mount technology) component. In this case it can be mounted on a PCB and ready to be used after mounting. All the electrical connections, mechanical protection and color conversion being already achieved.

In our approach we are looking into such package. To achieve this, some back end process is necessary after the epitaxial growth of GaN nanowires on a silicon substrate. The electrical contact must be redirected from the front side to the back side of the substrate and copper SnAg pad should be processed for an assembly ready chip.

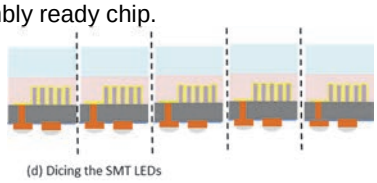

Figure 1 : LEDs ready for assembly after wafer dicing

Figure 1 illustrates this process. In order to achieve such chips some technological challenges must be overcome. The TSV may be fabricated before the front end process, that is the nanowires fabrication, or after, which is referred in this case as TSV-Last technology. The TSV-Last approach was extensively studied at LETI [2] and was developed for the packaging of CMOS image sensor [3, 4]. It typically deals with 60µm diameter and 120µm deep vias. In our case, copper filled, 70µm deep vias, 15µm in diameter were processed with the TSV-Last approach. The dimensions of the TSVs were chosen to handle the current density required by the application, to reduce the thermal barrier of the silicon substrate after assembly and to ensure mechanical resistance after wafer thinning. The TSV is processed after wafer bonding and thinning down to 70µm, therefore all the process must remain below 200°C to be compliant with the bonding polymer. The polymer must properly filled the nanowire topography, and the TTV after bonding should remain below 5µm to ensure uniform Si thickness after thinning. Due to the high aspect ratio of the TSV and the impossibility of using a thermal oxide, the main challenge after the etching step is the wall isolation. 3µm SiON PECVD at 150°C was used to provide enough passivation throughout the depth of the TSV. Finally to remove the oxide at the bottom of the TSV to ensure an electrical contact with the front pad, an etch back processed is used. The process must be carefully controlled to fully remove the oxide layer at the bottom of the TSV while keeping enough oxide at the top, the edge and the sidewall of the TSV. This operation requires very good control and knowledge of the etching rate at the top and at the bottom of the TSV. Figures 2 (a) and (b) provide a picture of the bottom of the TSV before filling and after filling.

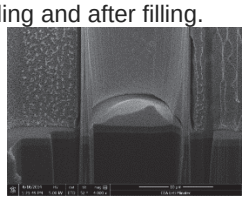
(a)
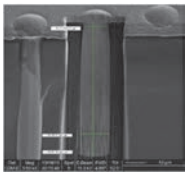
(b)

Figure 2: SEM picture of (a) the bottom of the TSV with oxide partially removed, (b) void free copper filled TSV

To achieve these different challenging processing steps, different process parameters were therefore tested and optimized on dummy wafers first. The etching rates of silicon, and oxide were determined using cross section and SEM imaging. A copper damascene electroplating bath was used to control the copper growth on the sidewall of the TSV to prevent void formation. The plating rate was slowed down for optimum filling, the results were again observed using cross section and SEM imaging.

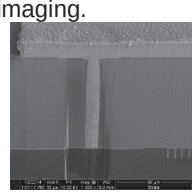
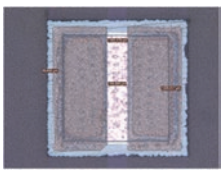

Figure 3: (a) SEM picture of a cross section with the final SnAg pad, the TSV and the encapsulated nanowires, (b) the back side of the chip before assembly

The complete process was successfully achieved on wafers with Si nanowires. While the wafers with GaN nanowires are still being processed, the results are very promising. This new wafer level approach offers an alternative to standard LED fabrication and packaging. Some key process parameters were studied and optimized to push the limits of TSV-LAST fabrication. Figure 3 (a) and (b) shows the chips at the end of the process, just before PCB mounting

Related Publications:
[1] *LED packaging, Mafket & Technology report*, Yole development, January 2013
[2] D. Henry, F. Jacquet, M. Neyret, X. Baillin, T. Enot, V. Lapras, C. Brunet-Manquat, J. Charbonnier, B. Aventurier, N. Sillon, "Through silicon vias technology for cmos image sensors packaging" *in Proc. IEEE Electronic Components and Technol. Conf. (ECTC)*, Lake Buena Vista, FL, May 27-30, 2008, pp.556-562
[3] D. Henry, J. Charbonnier, P. Chausse, F. Jacquet, B. Aventurier, C. Brunet-Manquat, V. Lapras, R. Anciant, N. Sillon, B. Dunne, N. Hotellier, J. Michailos, “Through Silicon Vias Technology for CMOS Image Sensors Packaging: Presentation of Technology and Electrical Results” *in Proc. IEEE Electronics Packaging Technology Conf.* (EPTC), Singapore, December 9-12, 2008, pp 35-44.
[4] Volpert, M., Soulier, B., Borel, S., Ait-Mani, N., Gaugiran, S., Gasse, A., Henry, D., A Wafer Level approach for led packaging using TSV last technology, Proceedings - Electronic Components and Technology Conference (Art. N° 7159732, 2015)

Optical efficiency characterization of LED phosphors using a double integrating sphere system

Research topic: Solid state lighting

P. Gorrotxategi, M. Consonni, A. Gasse

Abstract: We report on the methodology and implementation of a robust and accurate double integrating sphere system for measuring the absolute photoluminescence quantum yield and its temperature dependence for commercially available phosphors. The potential of our instrument for the examination of light interaction with samples of different absorption and scattering coefficients is also presented, as optical properties of luminescent materials have a major impact on the efficiency of LED's packaging. Our work gives special attention to the control and the optimization of light losses in the optical system in order to ensure reliable measurements.

Context and Challenges

Accurate characterization of phosphors used in LED for solid state lighting is essential to well understand the light extraction and conversion efficiencies of phosphor converted LED devices. However, very few studies addressing phosphor absolute luminescence quantum yield values and measurement methodologies can be found in literature. This work presents for the first time a detailed methodology for measuring absolute photoluminescence quantum yields of solid phosphors, carried out with a double integrating sphere system.

Main Results

In our setup, the sample is placed between two integrating spheres and illuminated by a blue laser module (450 nm, FWHM = 5 nm).

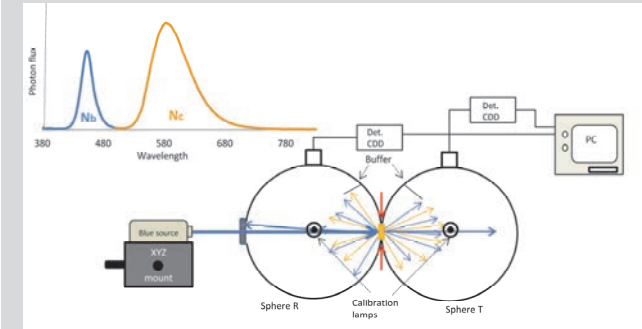

Figure 1 : Scheme of the double integrating sphere system

Reflected and transmitted lights are simultaneously measured with two spectrometers located in each sphere, which allows calculating the absolute photoluminescence quantum yield of the sample through:

$$QY = \frac{N_C}{N_B^{Abs}} = \frac{N_{CR} + N_{CT}}{N_B^{Inc} - (N_{BR} + N_{BT})}$$

In order to ensure reliable measurements, light losses in the system have been minimized by combining low-noise detectors, several calibration steps and a specific illumination bench test design for low backscattering. Samples were also thinned to limit scattering and edge losses. The uncertainty of the setup is found to be of the order of 3%, which is the state of the art of commercial equipment's.

Then, our instrument has been used to characterize several types of phosphor materials and to analyze the impact of phosphor concentration in a silicon matrix or temperature on both the emission spectrum and efficiency.

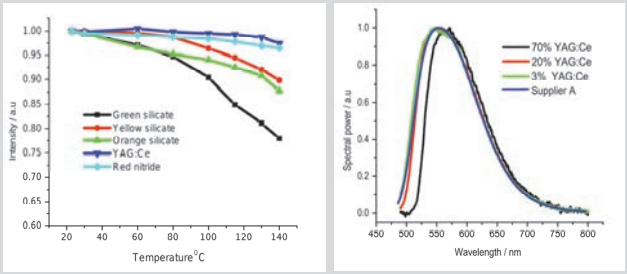

Figure 2 : Left, luminescence intensity decay of the studied phosphors with temperature. Right, red shift of YAG:Ce emission curve induced by high phosphor concentration.

As expected, YAG:Ce phosphor shows the highest luminescence quantum yield at 97% efficiency and an excellent temperature stability, while green silicate phosphor provides the lowest efficiency at 79%. Silicates phosphors are also found to loss up to 15% of luminescence intensity when temperature is raised to 140°C.
Due to the overlap between excitation and emission spectra, a red shift is also evidenced with phosphor concentration increase. For highly concentrated samples, this red shift is associated to a change in the spectrum shape as well as a loss of quantum yield, which highlights a strong self-absorption.

Perspectives

We have developed a robust instrument for the metrological evaluation of optical properties of solid luminescent samples. The choice of a double integrating sphere system allows accurate measurement of absorbed, reflected and transmitted light, providing valuable optical constants of the material.
A supercontinuum laser source will be soon implemented in order to better characterize the excitation spectra of phosphors. Scattering properties of phosphors at non-absorbing wavelengths will also be available.

Related Publications:
[1] Gorrotxategi et al., Journal of Solid State Lighting (2015) 2:1

05

DISPLAYS COMPONENTS

- OLED micro-displays technology
- OLED encapsulation
- GaN LED Micro-displays
- Visualization systems

Small-molecule-based photocrosslinkable fluorescent materials: towards multilayered and high-resolution emissive patterning

Research topic: Organic Light-Emitting Diodes

S Olivier*, L Derue, B Geffroy**, T Maindron, and E Ishow***
(*CEISAM–UMR CNRS 6230, Universite´ de Nantes, France,/ **CEA-Saclay, Gif-sur-Yvette, France)

Abstract: Solution-processable green and red-emitting molecular fluorophores possessing photopolymerizable acrylate units have been synthesized. Despite competitive energy transfer occurring between the excited photoinitiator and the radiative excited state of red-emitting materials, up to 40% of the initial thickness could be achieved after development. Multicolored stacked films with high optical quality have been fabricated. Resolved patterns as narrow as 600 nm could be obtained upon photolithography performed under an air atmosphere. High adhesion of the photocrosslinked materials on surfaces makes the resulting emissive thin films suitable for the realization of OLEDs [1].

Context and Challenges

Fluorescent micropatterns out of organic materials have recently received considerable attention in the fields of optical data storage [2], biosensors [3], organic lasers [4], organic light emitting diodes (OLEDs) [5] and counterfeiting [6]. For its OLED activity, our department has developed a collaboration with the CEISAM laboratory in Nantes to study the use of photo-crosslinkable R, G, B emitting molecules into OLED. The fine patterns could allow the realization of a new generation of microdisplays for which making individual R, G, B emitting OLED is impossible by standard shadow masks technology.

Main Results

The UV-vis absorption spectra of the green emitter (compound 7) onto Fig. 1 display very similar features in toluene solution and thin films, namely two overlapping bands at 370 nm and 354 nm. The absence of significant broadening or energy shift when passing from solution to solid thin films demonstrates weak π-π packing in the ground state due to steric repulsion induced by the bulky substituents (chemical structure of the compounds could be found in the publication [1]). Similar results have been found for the red compound 8. No blue compound has been made because it was impossible to get it crosslinked.

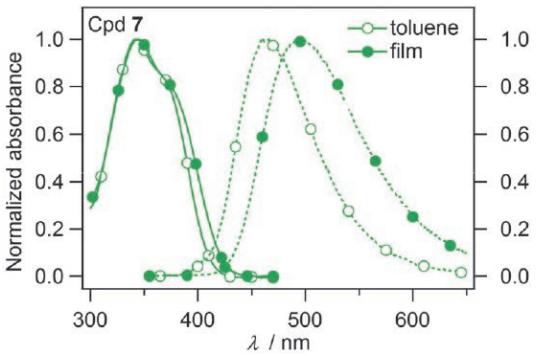

Figure 1 UV-vis absorption (solid symbols) and emission spectra (empty symbols of green-emitting compound (a) in toluene solution (5 x 10^{-5} mol L^{-1}), (b) processed as thin films from a 1 wt % solution in chloroform (130 nm).

The fluorescence quantum yields Φ_f using an integrating sphere for solid state measurements were valued at 0.36 for both compounds 7 and 8 processed as thin films. No drop in the emission intensity when going from solution to thin films was thus observed for compound 7 whereas a significant increase was detected for 8 (Φ_f in toluene was found at 0.29) as a result of restricted non-radiative processes provided by structural rigidification in the solid state.

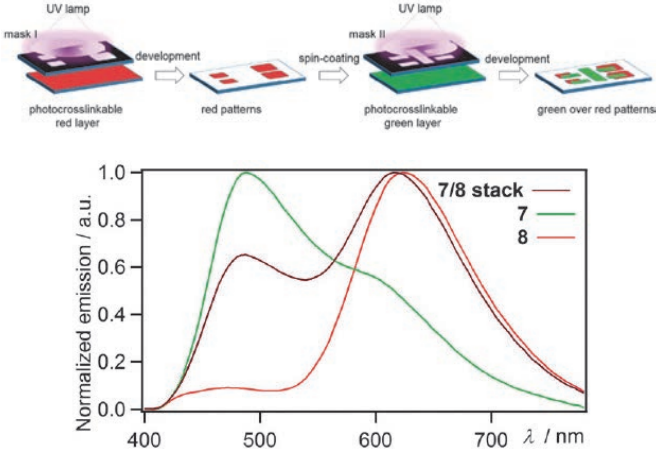

Figure 2 (top) Schematic description of the two-step photolithography process using two distinct photomasks and (bottom) resulting emission spectra of the green patterns, red patterns and superimposed green and red areas (λ_{irr} = 365 nm)

It was possible to photo-pattern the two compounds one on top of the other in order to demonstrate the possibility to realize R+G emission under UV irradiation (Figure 2). At the end, these compounds have been integrated as emitter materials in an OLED architecture. Performances of the red OLED have been measured to be 150 cd/m² below 8 V with a maximum current efficiency of 0.35 cd/A. Despite this apparently modest value, it is worth noting that the EL performance of the solution-processed OLED device actually represent the highest one ever reported for OLEDs fabricated following an all-solution deposition approach up to the ETL (Electron Transporting Layer) and incorporating non-doped photo-crosslinkable fluorescent materials as an emissive layer.

Perspectives

Further experiments to transfer this concept of an all-solution-processed OLED to acrylate-based small fluorophores, displaying optimized luminance and charge transport properties, are currently under progress to achieve higher OLED performance.

Related Publications:
[1] S. Olivier, L. Derue, B. Geffroy, T. Maindron and E. Ishow J. Mater. Chem. C, 2015, 3, 8403
[2] M. Irie, T. Fukaminato, T. Sasaki, N. Tamai and T. Kawai, Nature, 2001, 420, 759
[3] M. J. Hynes and J. A. Maurer, Mol. BioSyst., 2013, 9, 559–564
[5] S. Chenais and S. Forget, Polym. Int., 2012, 61, 390–406
[5] C.D.Muller, A. Falcou, N. Reckefuss, M. Rojahn, V.Wiederhirn, P. Rudati, H. Frohne, O. Nuyken, H. Becker and K. Meerholz, Nature, 2003, 421, 829–833
[6] B. Duong, H. Liu, C. Li, W. Deng, L. Ma and M. Su, ACS Appl. Mater. Interfaces, 2014, 6, 8909–8912

Defect analysis in low temperature atomic layer deposited Al_2O_3 and physical vapor deposited SiO barrier films and combination of both to achieve high quality moisture barriers

Research topic: Organic Light-Emitting Diodes, encapsulation, defects

T Maindron, T Jullien, and A André

Al_2O_3 and SiO films' single barriers as well as hybrid barriers of the Al_2O_3/SiO or SiO/Al_2O_3 have been deposited onto single 100 nm thick AlQ_3 organic films. The defects in the different barrier layers could be easily observed as non-fluorescent AlQ_3 black spots, under ultraviolet light. It has been observed that all devices containing an Al_2O_3 layer present a lag time τ from which defect densities of the different systems start to increase significantly. The best encapsulation solution, Al2O3/ SiO shows a large lag time of 795 h and a very low defect growth rate of 0.032/cm^2/h ($t>\tau$).

Context and Challenges

The Holy Grail for encapsulation of fragile organic optoelectronic devices [organic light-emitting diodes (OLED), organic photovoltaics, and organic thin film transistors (OTFT)] consists in the addition of vacuum deposited thin mineral barrier such as oxides, nitrides, or oxinitrides layers directly onto the organic circuit. This technology is today's so called thin-film encapsulation (TFE). In this context, our laboratory has provided several studies related to the investigation of defects in ALD-deposited Al_2O_3 barrier layers used to encapsulate OLED [2,3]. The technology basics is somehow similar to the one encountered in the world of food packaging, where barrier materials such as Al, Al_xO_y, or SiO_x are vacuum-deposited onto the plastic sheet surfaces, which act as barrier layers against moisture and oxygen. The main challenge today for organic optoelectronics is to achieve Thin-Film Encapsulation with ultrahigh barrier grade in order to allow a robust encapsulation with water vapor transmission rate (WVTR) ~10^{-6} g/m²/day necessary for OLED devices. Such achievements will open the way for the realization of lightweight, flexible OLED displays.

Main Results

Two different devices have been compared in this study (they are 4 in the original paper). They have been described below:

- Device A1: Si/AlQ_3 (100 nm)/SiO (25 nm)
- Device A2 : Si/AlQ_3 (100 nm)/Al_2O_3 (20 nm)/SiO (25 nm)

Figure 1 shows the evolution of the defects, seen as black spots appearing onto the AlQ_3 film under UV light [2], for device A1.

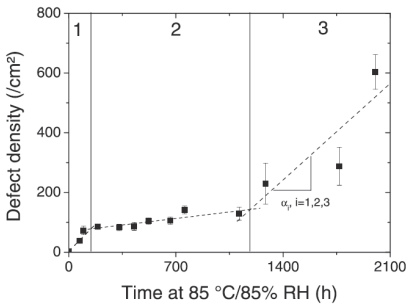

Figure 1 Defect density evolution vs storage time for device A1: 1, 2, and 3 represent the three regimes of defect growth; α_i represents the slope of the linear fit of data in the different regimes 1, 2, and 3.

It can be seen that the defect growth rates for device A1 are threefold depending on the storage time. There is no lag time for the occurrence of defects. At the end, the total defect density is very high, 600 /cm² coherent with the pinhole-full nature of PVD-deposited SiO films.

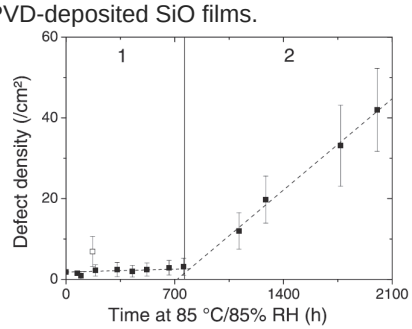

Figure 2 Defect density evolution vs storage time for device A2: 1 and 2 represent the two regimes of defect growth

Figure 2 shows the evolution of the defects for device A2. Contrary to device A1, it can be seen that defect growth rates are far lower than device A1 ones. At the end of the test, the total defect density has been estimated to be only 50 /cm². This good result has been allowed thanks to the addition of an Al2O3 barrier layer, deposited at low temperature ALD, underneath the SiO layer. At the end, the PVD layer acts as a passivation layer that prevents accelerated degradation of the Al_2O_3 layer. Most importantly, a large lag time of 750 h has been observed confirming the high stability of the Al_2O_3/ SiO material to hot humid atmospheres. A very low WVTR (Water Vapor Transmission Rate) has been estimated to be 1.6x10^{-6} g/m²/day which turns out to be one of the best WVTR at 85 °C/85% RH measured in the literature.

Perspectives

Further experiments to implement this concept of Al_2O_3 passivation by means of another materials will be investigated through the use of TiO2 deposited by low temperature ALD. Doing that a complete fully integrated ALD barrier could be used instead of an hybrid ALD/PVD one. Further implementation onto OLED devices will be done.

Related Publications:
[1] T. Maindron, T. Jullien, and A. André, J. Vac. Sci. Technol. A, 2016, 34, 031513
[2] T. Maindron, T., B. Aventurier, A. Ghazouani, T. Jullien, N. Rocha and J.-Y. Simon Thin Solid Films, 2013, 548, 517-525
[3] T. Maindron, B. Freiburger and T. Jullien, AVS ALD2015, 2015, poster

Progress towards emissive, ultra-high-brightness GaN LED microdisplays

Research topic: emissive microdisplays, GaN LEDs, high-brightness, augmented reality

F. Templier, L. Dupré, E. Tirano, B. Aventurier, F. Marion, JM Bethoux, M Lacroix, M, Marra, V Verney, L Dupré, F Berger, W Ben Naceur, A Sanchot, I.C Robin, M.A di Forte-Poisson*, P Gamarra*, C Lacam* and M Tordjman* (* III-V Lab, Palaiseau, France)

Abstract: High-brightness GaN-based emissive microdisplays can be fabricated with different approaches. Using the hybridization approach, we have developed monochrome passive-matrix GaN microdisplay prototypes, with dimensions of 300 x 252 pixels and a pixel pitch of 10 µm. Brightnesses as high as 1 x 10^6 and 1 x 10^7 Cd/m² were reached for blue and green arrays, respectively. The technology is suitable for augmented reality systems and Head-Up Displays

Context and Challenges

The growing interest for wearable devices has highlighted the need for high-performance microdisplays. Such displays are currently based on technologies such as liquid-crystal displays (reflective or transmissive), organic LEDs (OLEDs), or MEMS-based devices like micro-mirror arrays (digital light processing) and laser-beam steering (LBS). Emissive microdisplays such as OLEDs are particularly attractive for these applications. However, for some applications such as see-through glasses, or head-up displays, a brightness of 5000 Cd/m² or more is needed, which exceeds the possibilities of OLED microdisplays. A new type of emissive display, using GaN, has been proposed to provide a drastic improvement of the brightness while maintaining excellent contrast and compactness [1, 2]

Main Results

We have developed blue and green, 300 x 252 pixels, passive-matrix GaN microdisplays with very high brightness [3]. Figure 1 shows the green device powered-up on the electronic card. The inset shows group of activated pixels. Each pixel consist of one 6.5 x 6.5 µm microled, with a pitch of 10 µm. Another inset shows a group of pixels on a blue-emitting device.

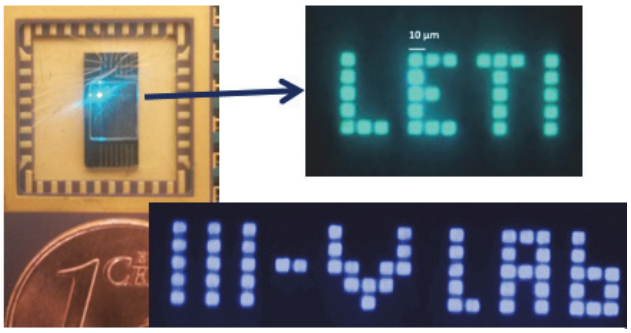

Figure 1: High brightness green and blue GaN microdisplays [3]

Electro-optical characterization has been carried out on single pixels of the above-mentioned passive-matrix 10µm-pitch hybridized arrays. Characteristic of a blue-emitting pixel is shown on Figure 2, with the plot of brightness as a function of driving current. Optical power reaches 100 µW for a driving current of 1 mA, which corresponds to a brightness of 4 x 10^6 cd/m². This level of luminance is several orders of magnitude higher than those of OLED or other types of microdisplays. Characteristic of a green-emitting pixel is also shown on Figure 2. A brightness of 2.2 x 10^7 cd/m² is obtained from the LED array at 1 mA. This is much higher than blue device despite lower optical power (21 µW), thanks to better eye sensitivity in the green.

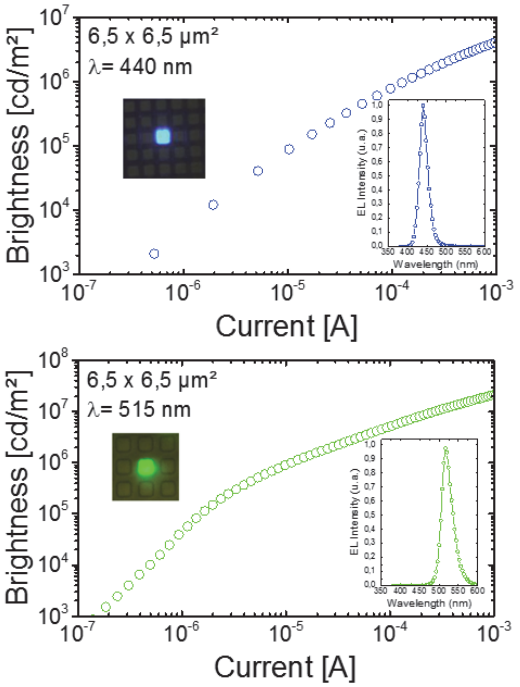

Figure 2: Brightness of Blue and Green single pixels.

In summary, we have developed blue and green 10-µm pitch arrays with very high brightness.

Perspectives

These results show that the developed technology is very promising for the fabrication of high resolution, small pixel-pitch, high-brightness GaN-based emissive microdisplays. The next step is to fabricate a full active-matrix GaN microdisplay. We are now developing an 873 x 500 pixel, 10 µm-pitch, active –matrix, monochrome GaN Display.

Related Publications:
[1]J. Day, J. Li, D. Y. C. Lie, C. Bradford, J. Y. Lin and H. X. Jiang, Appl. Phys. Lett., 99, p031116 (2011),
[2] F. Templier et al. "High-Brightness GaN LED Arrays Hybridized on Silicon Interconnect at a Pixel Pitch of 10 µm", The 21st International Display Workshops in conjunction with Asia Display 2014 (IDW/AD'14), December 3-5 2014, Niigata, Japan (2014),
[3] F. Templier, J-M. Bethoux, B. Aventurier, F. Marion, S. Tirano, M. Lacroix, M. Marra, V. Verney, L. Dupré, F. Olivier, F. Berger, W. Ben Naceur, A. Sanchot, I-C Robin, M-A di Forte-Poisson, P. Gamarra, C. Lacam, M. Tordjman, "Blue and Green 10-µm pixel pitch GaN LED Arrays with very high brightness", Invited Talk, The 22nd International Display Workshops 2015 (IDW'15), December 8-11 2015, Otsu, Japan (2015).,

Color solutions for high-brightness GaN LED arrays for display application

Research topic: emissive microdisplay, color conversion, color generation, GaN LEDs

A. Sanchot, M. Consonni, S. Le Calvez, I.C. Robin, P. Gamarra*, F. Templier
(* III-V Lab, Palaiseau, France)

Abstract: Color is a big challenge for high-brightness GaN-based microdisplays. We evaluate two approaches: direct generation (multiple-emission stack of MQWs) and color conversion (with Quantum dots). We have obtained very encouraging results in both ways, including a very saturated Red color using QD color conversion.

Context and Challenges

For some new applications such as see-through glasses, or head-up displays, a brightness of 5000 Cd/m² or more for the microdisplay is needed, which exceeds the possibilities of existing OLED microdisplays. A new type of emissive display, using GaN, has been proposed to provide a drastic improvement of the brightness while maintaining excellent contrast and compactness [1]. For such displays, the LED structure normally emits a single wave length, therefore color is a key challenge for this new kind of displays. We here report results on two different approaches for making color microdisplays.

Main Results

Color can be obtained by direct generation of the three components, or by using a single emission wavelength and color converters. We are investigating the two approaches. For the first one, our partners at 35 Lab evaluate the stacking of the three components. In a first step, we evaluate dual wavelengths Blue and Green InGaN/GaN Multi Quantum Wells (MQWs) [2].

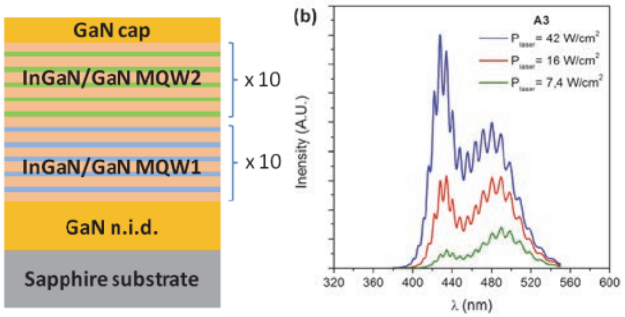

Dual-wavelength Blue and Green stacks: structure (left) and photoluminescence response (right)

Such structure (figure) has been developed and evaluated. The photoluminescence response under different incident power shows an emission shift from blue towards green. This first result is encouraging and we are now developing full LED structures.

We also evaluate the use of color conversion for making color displays. It consists of using blue emission and down converting it into Green or Red by photoluminescence using phosphor materials. In our approach, we actually use Quantum Dots (QDs) converters. Such materials absorb and emit at different wavelengths, depending on their chemical composition and size. The emission peak is very narrow (around 30nm) which makes them very suitable to obtain high color saturation. We have first evaluated QDs for the conversion in Red. Here QDs are core-shell CdSe/ZnS quantum dots with an emission wavelength at 620nm. In our experiment, we have deposited QDs on Blue a emitting 10µm-pitch, LED array hybridized on silicon circuit (Figure: top). We have measured emission without (left) and with (right) red converting QDs.

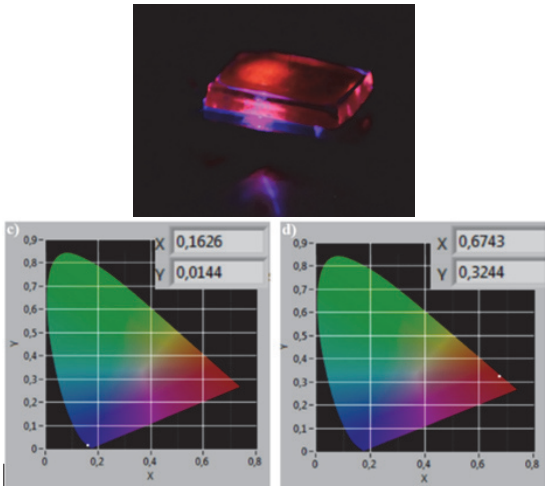

Color conversion with QDs ; structure (top) and results on chromaticity diagram (bottom: see white dot for color coordinate)

Without converter, the emission is a highly saturated blue. With QD converter, the color coordinates correspond to a highly saturated red (X=0.67; Y = 0.32). To our knowledge, this is the best color conversion result obtained so far.

Perspectives

Work on color conversion now continues with the green conversion and also the patterning of these QDs.

Related Publications:
[1] J. Day, J. Li, D. Y. C. Lie, C. Bradford, J. Y. Lin and H. X. Jiang, Appl. Phys. Lett., 99, p031116 (2011),
[2] Piero Gamarra, Cédric Lacam, Maurice Tordjman, François Templier and Marie-Antoinette di Forte-Poisson, "Dual wavelengths InGaN/GaN MQW and LED structures", 16th European Workshop on Metalorganic Vapour Phase Epitaxy (EWMOVPE XVI), June 7 – 10, 2015, Lund, Sweden
[3] Audrey Sanchot, Marianne Consonni, Stéphanie Le Calvez, Ivan C. Robin, and François Templier, "Color conversion using red Quantum Dots integrated in a sol-gel on high-brightness blue GaN LEDs". Proc. of 2015 MRS Spring Meeting , April 6-10, 2015, San Francisco, California (2015),

Holographic display for extended informative windshield

Research topic: Head Up Display, Head Mounted Display, Holographic Display, Augmented Reality

C Martinez, U Rossini, D Sarrasin

Abstract: We present the development of a windshield display system based on the use of a Head Mounted Projection Display (HMPD) and a transparent holographic screen designed to allow a light efficiency optimized visual rendering.

Context and Challenges

The field of view and the eye position limits (eye box) are the main limitations in the development of Head Mounted or Head Up Displays (HMD & HUD).To deal with these constraints, sophisticated optical designs must be elaborated so that HMD and HUD have been limited so far to very specific aircraft military applications [1]. Recent progress in the field of ICT has led to an increase of the information flow towards general users, and HMD and HUD are now also been studied in a broad range of applications from automotive industry to Augmented Reality consumer markets.

CEA Tech has developed a smart windshield in collaboration with Optsys, a French company specialized in vision equipment for armored vehicles and Hologram Industries Research [2]. This alternative visualization solution is based on a Head Mounted Projection Display (HMPD) concept [3] and has required the development of a transparent holographic projection screen.

Main Results

Figure 1a shows the system specification with a projector and an orientation/gesture sensor mounted on the user helmet. When looking downwards, the HMPD detects a pictogram that enables a dashboard projection (fig. 1b). When looking upwards, a different pictogram enables an AR functionality (e.g. drone detection).

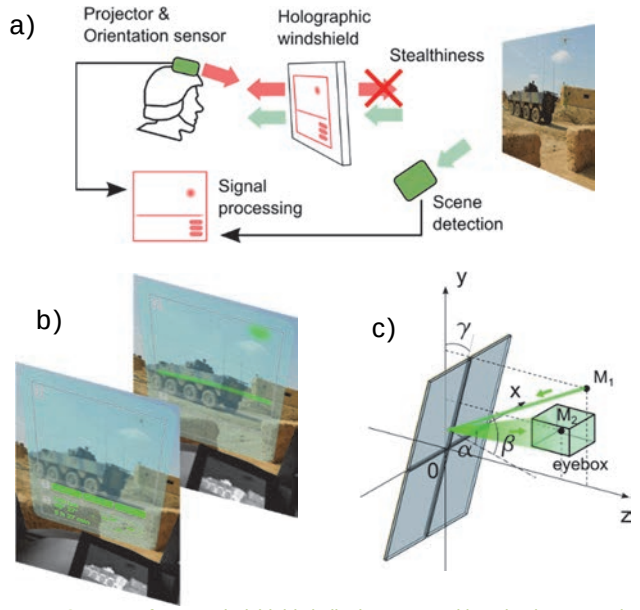

Figure 1: Concept of smart windshield a) display system, b) projection scenario, c) holographic screen geometric characteristics

Transparent projection screen is a challenging development as the device must enable mixing of both transparency and diffusion. Our laboratory has developed in collaboration with Hologram Industries Research a holographic windshield dedicated to a specific projection and viewing geometry.

Figure 1c shows the holograms that form the smart windshield. Each four holograms is recorded with respect to a projection point reference M1 and a viewer location M2 in a given eyebox.

Figure 2a shows the HMPD developed at Leti with a DLP projector and a compact camera. The DLP lighting electronic has been modified to enable a constant green LED power supply (red and blue LEDs are inactivated) leading to about 30 Lum around 532 nm.

Figure 2b shows the visual result of a projection on the windshield. In usual viewing condition, measured brightness is 210 Cd/m².

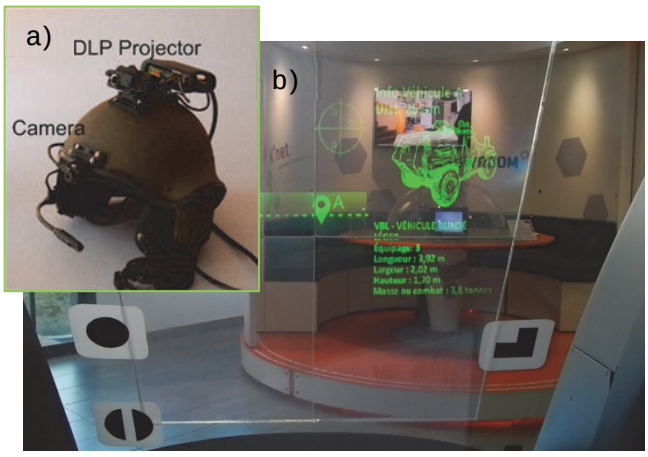

Figure 2: Photography of the system: a) The HMPD helmet developed by the laboratory, b) a real view of the projected information (green) on the holographic windshield

Perspectives

The HMPD holographic windshield concept has been successfully implemented in a demonstration vehicle of Optsys to exhibit high luminosity of the display on an extended transparent surface while maintaining the stealth of the vehicle, superposition of information in accordance with the outer scenery and the head orientation of the pilot enabling interactive AR applications. Research now focuses on the increase of the screen brightness for more enhanced external glaring light conditions and on the design of polychromatic display solutions.

Related Publications:
[1] J. E. Melzer, F. T. Brozoski, T. R. Letowski, T. H. Harding, and C. E. Rash, “Helmet Mounted Displays: Sensation, Perception, and Cognition Issues”, pp. 805–848, US Army Aeromed. Res. Lab., Fort Rucker, AL
[2] C. Martinez, U. Rossini, S. Denis, M. Lechevin, G. Dausmann, Z. Yang, and M. Krug, "Holographic Display for Extended Informative Windshield," in Imaging and Applied Optics 2015, OSA Technical Digest (online) (Optical Society of America, 2015), paper AIW4C.2.
[3] Jannick P. Rolland, Frank Biocca, Felix Hamza-Lup, Yanggang Ha, and Ricardo Martins, “Development of Head-Mounted Projection Displays for Distributed, Collaborative, Augmented Reality Applications”, Presence: Teleoperators and Virtual Environments 2005 14:5, 528-549.

06

OPTICS AND NANOPHOTONICS

- Thin film Fabry-Perot filter arrays
- Metal - dielectric multilayer IR filters
- Topological insulator structures

Multispectral interference filter arrays with compensation of angular dependence or extended spectral range

Research topic: Multilayer interference filters, Multispectral detection, Visible and Near-infrared

L Frey, L Masarotto, M Armand, M-L Charles, and O Lartigue

Abstract: Thin film Fabry-Perot filter arrays with high selectivity can be realized with a single patterning step generating a spatial modulation of the effective refractive index in the optical cavity. We investigate the ability of this technology to address two applications in the field of image sensors. First, the spectral tuning may be used to compensate the blue-shift of the filters in oblique incidence, provided the filter array is located in an image plane of an optical system with higher field of view than aperture angle. The technique is analyzed for various types of filters and experimental evidence is shown with copper-dielectric infrared filters. Then, we propose a design of a multispectral filter array with an extended spectral range spanning the visible and near-infrared range, using a single set of materials and realizable on a single substrate.

Context and Challenges

In this study, we investigate the potential of the dielectric nanostructuration technology to address two major issues of interference filter arrays, focusing on the field of VIS and NIR image sensors.

Compensation of blue-shift under oblique incidence with nanostructured filters

The first issue is the blue-shift under oblique incidence, one major usual drawback of interference filters. Rather than suppressing the angular dependence, we propose a simple technique to compensate for it when the incidence angle is variable over the filter surface, for example in the image plane of an imaging system with low aperture compared to the chief ray angle. The red-shift results from the increase of the effective refractive index of the layer within the filter stack which is the most sensitive to refractive index changes. This layer is realized by nanostructuring a first dielectric material and gap-filling with another dielectric material with a different refractive index. We realized a demonstrator with Cu filters, patterned SiN and gap-filling with SiO2 to show that accurate compensation can effectively be achieved with standard semiconductor manufacturing tools, and independently of the fine tuning of the nominal spectral response. Therefore, this technique for blue-shift compensation is robust regarding layer optical constants and thicknesses. The main technological requirement is the control of lateral dimensions in the patterning process. The key point of the effective index method is its simple technological implementation with a single patterning step even when a number of intermediate corrections are desirable, providing gradual compensation of the blue-shift.

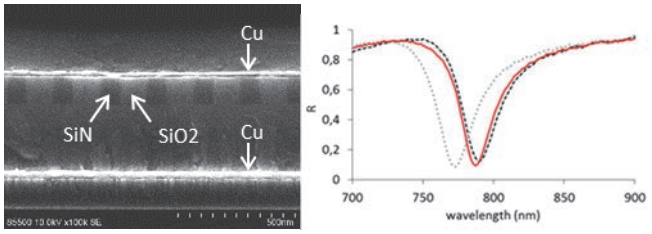

SEM cross section of the nanostructured filter, and measured reflectance in normal incidence (dark dashed line), at 25° incidence (grey dotted line), at 25° with blue-shift compensation (red line).

The technique is applicable for both high and low index spacers, for Fabry-Perot designs based on metallic or Bragg mirrors, and also for non Fabry-Perot interference filters. It is therefore possible to design narrower band-pass filters for 3D active imaging, allowing higher distance measurement range, or lower power consumption and lower cost of the light source. It is also possible to compensate the blue-shift of the cut-off wavelength in IR-blocking filters, and suppress the color shading in highly demanding imaging applications.

Multispectral Fabry-Perot filters with extended spectral range

The second issue is the extent of the spectral range of multispectral filter arrays over the whole VIS and NIR range, using a single set of materials to minimize the process complexity. Our solution advantageously combines the variations of layer thickness and refractive index to increase the spectral range while minimizing the number of patterning steps. One single etching step with sub-wavelength patterns proves to be necessary whatever the number of filters, or two if a higher selectivity is desired. Here also, the robustness regarding layer thicknesses is a key advantage of the process. This technology may be suitable for manufacturing multispectral filter arrays with high selectivity in a monolithic or hybrid integration on a number of devices such as image sensors or displays. The technology is compatible with a small pixel size, typically 1µm, since the total thickness of the filters is 0.3 to 0.7µm. The simplicity of the process is particularly advantageous over a pure staircase approach as soon as more than three different filters are required, as in RGBIR imaging or multispectral imaging.

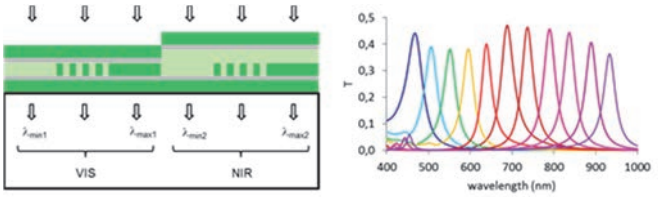

Cross section sketch of multispectral FP filter array with extended range in VIS and NIR range, simulated transmittances on glass of multispectral Ag/TiO2/SiO2 FP filters with single-cavity architecture

Related Publications:
[1] L. Frey, L. Masarotto, M. Armand, M.L. Charles, O. Lartigue, « Multispectral interference filter arrays with compensation of angular dependence or extended spectral range », Opt. Expr. 23, 11799 (2015)

Multispectral detection with metal-dielectric filters: an investigation in several wavelength bands with temporal coupled-mode theory

Research topic: infrared filters, frequency selective surfaces

E Lesmanne, R Espiau de Lamaestre, S Boutami, C Durantin, L Dussopt and G Badano

Abstract: New developments in infrared imaging include the need for simultaneous multispectral detection to get more information from the scene. Pixel-level filtering has not been sufficiently investigated as a means to achieve that goal. We deal with filters based on arrays of slit apertures in a metallic layer and describe their performance in terms of maximum transmission and lineshape. As a tool for this discussion, we develop an approach based on the temporal coupled mode theory, which models the filter as a set of resonators interacting with their environment via loss channels.

Context and Challenges

Multispectral imaging has a variety of applications in astronomy, space and defense systems. An inexpensive way to achieve asynchronous spectral sensitivity is to use a filter wheel, placed between the focal plane array detector and the scene, away from the focal plane array. For synchronous multiband detection, the Bayer mosaic approach, where each pixel of the focal plane array is functionalized with a separate filter, has not received sufficient attention. It is however very interesting in terms of flexibility and implementation costs.

The current fabrication technique of infrared filters, based on multilayer dielectric stacks, is difficult to transpose to the pixel level. To allow wavelength selection, the stack must be varied from a pixel to the next, a difficult feat in small pixel pitch detectors. The structures we benchmark are based on arrays of subwavelength apertures lithographically patterned in a thin metallic layer. One can vary the resonant wavelength by acting on the aperture size, without it being necessary to change the thickness of the metal.

Main Results

We develop an analytical model based on the temporal coupled-mode theory. It models the filter as a resonator interacting with its environment via ports (see Fig. 1). These interactions are described by loss rates γ_1 and γ_2, which sum is the radiative loss rate γ_{rad}. The metallic absorption is described by an absorption loss rate γ_{abs}. These loss rates allow describing the transmission of the system, as shown by Eq. 1.

$$T = \frac{\gamma_{rad}^2}{(\omega - \omega_0)^2 + (\gamma_{rad} + \gamma_{abs})^2} \qquad (1)$$

Knowing the loss rates, we have access to an insightful information about the transmission at resonance and the full width at half maximum (FWHM), two parameters describing the transmission spectrum.

We find analytical expressions of these loss rates for a specified geometry, namely periodical rectangular apertures in a metal layer [1]. These expressions include both geometrical parameters and material parameters like the optical indexes. Comparisons with Finite Difference Time Domain (FDTD) simulation results have been performed in order to check the validity of our model.

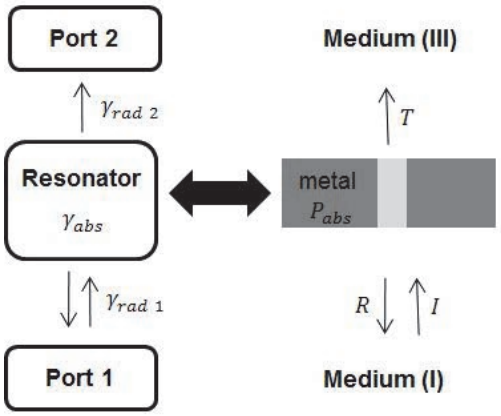

Figure 1: Temporal coupled-mode theory model (left) of the real system, a rectangular aperture in a metal layer (right). I is the incident wave, R the reflected wave and T the transmitted wave.

This model can be used to optimize the geometry of the structure, for example by investigating the link between maximum transmission and FWHM [1, 2] or comparing different metals [3].

It allows one to better apprehend the strengths and limitations of frequency selective surfaces in the infrared domain. Although it does not provide the accurate resonant wavelength, it does predict the correct loss rates, which can be injected in a temporal coupled mode theory formalism to obtain the transmission linewidth, for any combination of slit size and materials.

Perspectives

The use of these structures as filters is limited by a tradeoff between the linewidth and the maximum transmission, for a given resonant wavelength. In perspective, our model can be extended to cover a wider range of wavelengths and describe the effect of metallic loss on the filtering efficiency.

Related Publications:
[1] E Lesmanne ; L Dussopt and G Badano, Multispectral detection with metal-dielectric filters: an investigation in several wavelength bands with temporal coupled mode theory, II-VI Workshop (2015)
[2] E. Lesmanne, R Espiau de Lamaestre, S Boutami, C Durantin, L Dussopt and G Badano, Multispectral Detection with metal-Dielectric Filters: an Investigation in Several Wavelength Bands with Temporal Coupled Mode Theory, *Journal of Electronics Materials*, doi: 10.1007/s11664-016-4475-8 (2016)
[3] Communication at OPTRO 2016: E. Lesmanne, Roch Espiau de Lamaestre, Salim Boutami, Cédric Durantin, Laurent Dussopt and Giacomo Badano, Infrared Multispectral Detection With Metal-dielectric Filters: A Model Based On The Temporal Coupled Mode Theory

Quantum Transport in HgTe/CdTe Topological Insulator Structures

Research topic: Topological Insulator, Quantum Hall Effect,

C Thomas, O. Crauste*, C. Bauerle*, P. Ballet and T. Meunier*
(* Institut Néel, CNRS, Université Joseph Fourier, Grenoble, France)

Abstract: We report on quantum Hall-effect studies in gated strained-HgTe/CdTe topological structures. Two-dimensional Dirac fermion transport is demonstrated over HgTe surfaces with very high mobility and no parasitic bulk conduction. These results open up the way toward application of this topological material system for spintronics and topological superconductivity.

Context and Challenges

Topological Insulators (TI) are a new class of materials attracting great interest both theoretically and experimentally thanks to their unique electronic and spin properties that arise at their interfaces. With an inverted band structure, the semi-metal HgTe has been identified as a strong TI provided the opening of band-gap generated by growing tensile strained HgTe/CdTe structures [1]. Here we present results of low-temperature electronic transport over molecular beam epitaxy (MBE)-grown HgTe/CdTe interfaces, witnessing the high-quality HgTe material and the topological nature of its surfaces.

Main Results

Tensile-strained HgTe/CdTe structures with symmetric HgCdTe barriers have been grown by MBE and further processed into top-gated Hall bars for low-temperature electronic transport measurements (fig.1). Low magnetic field Hall investigation reveals very large carrier mobility in excess of $5.10^5 cm^2/V.s$ for a density of a few $10^{11}/cm^2$. Such a high mobility has been obtained after a careful optimization of HgTe surfaces and nano-fabrication process [2,3]. Figure 1 (c) also demonstrates the existence of a charge neutrality point with the change of sign in the Hall constant when scanning the strained gap from valence band hole transport (Vg<-0.6V) to high mobility electrons (Vg>-0.6V).

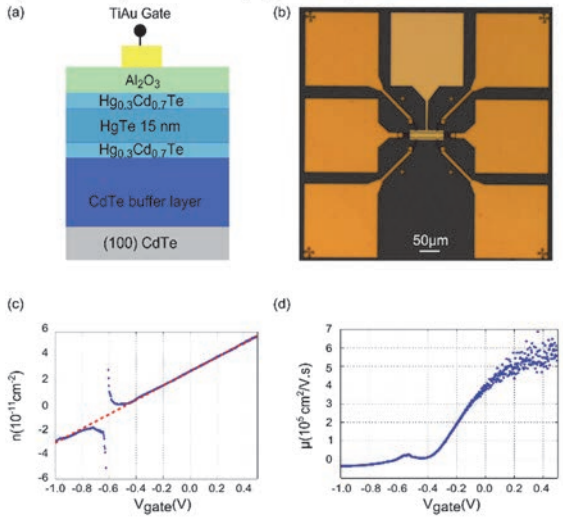

Figure 1 : HgTe/CdTe structure with gate and dielectric (a), and associated Hall bar (b). Resulting carrier density and mobility (c) and (d).

Quantum Hall effect signatures are displayed in Fig.2 in the form of detailed maps of the longitudinal and transverse resistances as a function of the gate voltage and the magnetic field. The data show clear evidence of conductance plateaus corresponding to the successive filling of Landau levels. These plateau are very well defined for electrons and are plotted as a function of the quantum of conductance (e^2/h) demonstrating integer filling factors. Associated to these Landau levels is the total vanishing of the longitudinal conductance, thus giving a direct evidence of the absence of bulk conduction within HgTe. This latter observation contrasts to the transport signatures of bismuth-based topological insulators characterized by a very strong intrinsic bulk conduction and a very low electron mobility.

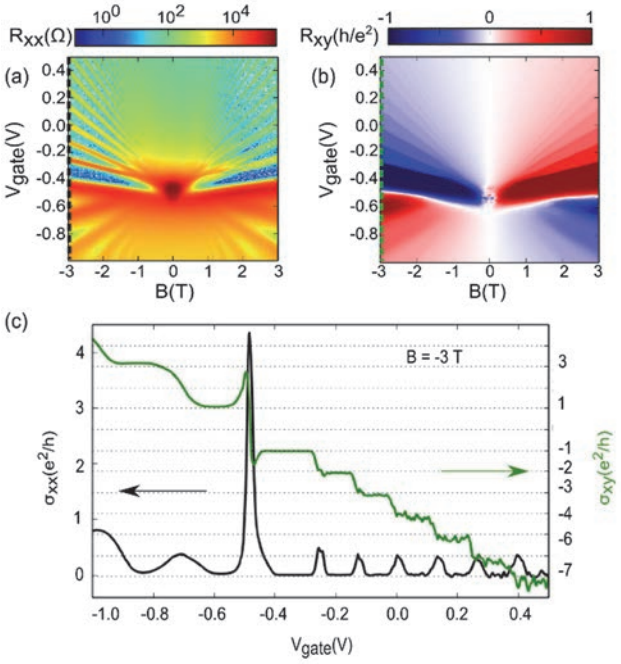

Figure 2 : longitudinal (a) and transverse (b) resistance mapping. Traces of conductance as a function of gate voltage for a given magnetic field (c).

Analysis of the fan diagram extracted from the odd filling factors provide direct evidence of a surface transport through direct fermions, thus clarifying the topological nature of this system.

Perspectives

With clear evidence of topological transport over HgTe surfaces, new developments can be envisioned to implement 3D topological insulators into real devices. Among the numerous options, spintronic elemental building-blocks such as filters or transistor, and proximity induced superconductivity are considered.

Related Publications:
[1] C. Brüne, X.C. Liu, E.G. Novik, E.M. Hankiewicz, H. Buhmann, Y.L. Chen, X.L. Qi, Z.X. Shen, S.C. Zhang and L.W. Mollenkamp, Phys. Rev. Lett. 106, 126803 (2011).
[2] P.Ballet, C.Thomas, X.Baudry, C.Bouvier, O.Crauste, T.Meunier, G.Badano, M.Veillerot, J.P.Barnes, P.H.Jouneau and L.P.Lévy, *J. Elec. Mat.*, 43, 2955 (2014).
[3] C.Thomas, X.Baudry, J.P.Barnes, M.Veillerot, P.H.Jouneau, S.Pouget, O.Crauste, T.Meunier, L.P.Lévy, P.Ballet, *J. Cryst. Growth* 425, 195 (2015).

07

PHD DEGREES AWARDED IN 2015

- Romain GIRARD-DESPROLET
- Simon OLIVIER
- Ujwol PALENCHOKE
- Justin ROUXEL
- Pierre TCHOULFIAN

Romain GIRARD-DESPROLET

PhD degree (Institut National Polytechnique of Grenoble, France)

PLASMONIC SPECTRAL FILTERING USING METALLIC NANOSTRUCTURES ENVISIONED FOR CMOS IMAGE SENSORS.

Image sensors have experienced a renewed interest with the prominent market growth of wireless communication, together with a diversification of functionalities. In particular, a recent application known as Ambient Light Sensing (ALS) has emerged for a smarter screen backlight management of display-based handheld devices. Technological progress has led to the fabrication of thinner handsets, which imposes a severe constraint on light sensors' heights. This thickness reduction can be achieved with the use of an innovative, thinnest and entirely on-chip spectral filter. In this thesis, we investigated and demonstrated plasmonic filters aimed for commercial ALS products. The most-efficient filtering structures were identified with strong emphasis on the stability with respect to the light angle of incidence and polarization state. Integration schemes were proposed according to CMOS compatibility and wafer-scale fabrication concerns. Plasmon resonances were studied to reach optimal optical properties and a dedicated methodology was used to propose optimized ALS performance based on actual customers' specifications. The robustness of plasmonic filters to process dispersions was addressed through the identification and the simulation of typical 300 mm fabrication inaccuracies and defects. In the light of these studies, an experimental demonstration of ALS plasmonic filters has been performed with the development of a wafer-level integration and with the characterization and performance evaluation of the fabricated structures to validate plasmonic solutions.

Simon OLIVIER

PhD degree (University of Nantes, France)

MATERIAUX PHOTORETICULABLES A BASE DE FLUOROPHORES PHOTO POLYMERISABLES: SYNTHESE ET CARACTERISATIONS POUR LA FABRICATION D'OLEDS.

This PhD work realized in co-supervision between the University of Nantes and the CEA-LETI in Grenoble aims at elaborating photopolymerizable emissive molecules to fabricate electroluminescent diodes following a solution process. Although many studies have been performed on the elaboration of photopolymerizable hole transporting layers to get rid of the commonly used evaporation processes, poorly compatible with large areas and expensive, little has been done on the wet deposition of emitting layers. The studies performed herein report on the syntheses, the characterizations, and the use of emissive small molecules, amenable to polymerize and form highly fluorescent amorphous thin films Monomers emitting in the blue, green and red ranges have been synthesized following a modular strategy involving the same key intermediate compound, thereby minimizing the synthesis steps. They yielded thin films with amorphous and electronic properties ruled independently by the substituant bulkiness and the increasing power of the electron-withdrawing group. After simple UV irradiation and development, nanometric insoluble thin layers, remaining fluorescent, have been obtained. Such photopolymerization has been harnessed to fabricate multilayer systems, after optimization of the exposure conditions, the photo-initiator concentration and the surrounding environment. Electroluminescent devices have been realized by coupling this wet deposition process (e.g. spin-coating and inkjet) with the vacuum evaporation of top layers, and their performances have been measured.

Ujwol PALENCHOKE

PhD degree (Institut National Polytechnique of Grenoble, France)

CONCEPTION AND REALIZATION OF SPECTRAL SORTER FOR INFRARED AND VISIBLE IMAGING SYSTEM.

The advancement and scaling effect in complementary metal oxide semiconductor (CMOS) and micro-electro-mechanical system (MEMS) technology has made possible to make smaller image sensors with higher density of imaging pixels to respond at the demand of low cost imagers. Generally, the higher pixel density in imaging system is achieved by shrinking the pixel size in an array. The shrinking of pixel size however deteriorates the optical efficiency. The signal to noise ratio (SNR) and dynamic range (DR) of imaging system decreases as pixel size decreases. This imposes the tradeoff between the performance and minimum achievable pixel size. As the pixel size continues to decrease and approach the dimensions comparable to the wavelength, the spectral separation techniques used in current generation imaging system should be revised. New design methodologies have to be explored to cope with optical efficiency issues.
This dissertation explored different concepts to separate or sort specific wavelengths to design optically efficient pixels. We focus our study in Far Infrared (8µm - 12µm) and visible (0.4 µm – 0.7 µm) spectrum which are mainly used for thermal and visible imagery respectively. We introduced the concept of spectral sorting based on normalized optical efficiency (NOE). For given number of pixels (N) or detectors, we define the spectral sorting if NOE of individual pixels, considering incidence power from all pixel domain, is greater than 1/N. We study CMOS compatible differently sized optical patch antenna to efficiently sort the infrared light using numerical techniques. Using array of patch antennas the near perfect absorption of multiple wavelengths in infrared spectrum was studied experimentally. We also explored dielectric based sorting structure for visible spectrum. The thesis presents the strategy to design sorting structure for visible spectrum which could leads to optical efficiency as high as 80% in pixel size as less as 0.5µm.

Justin ROUXEL

PhD degree (University of Reims, France)

DESIGN AND REALIZATION OF MINIATURIZED PHOTOACOUSTIC CELLS FOR TRACE GAS DETECTION.

Photoacoustic cells are optical sensors based on the absorption of photons by gas molecules. The pressure wave created by gas relaxation is proportional to the trace gas concentration. Furthermore the photoacoustic signal is inversely proportional to the cell volume. Thus cell miniaturization can improve performances and enables the integration of the cell on a lab-on-a-chip and its development for detection of greenhouse or toxic gases. This work consists in designing, realizing and characterizing miniaturized photoacoustic cells, based on the differential Helmholtz resonator (DHR) principle. In a first phase, modeling by the finite element method of millimeter scale cells has shown that the miniaturization of this type of resonator should effectively improve the detection limit. Thus, the ambitious realization of a DHR cell on silicon by the use of microelectronic techniques has been attempted. However, this extreme miniaturization direction encountered design and fabrication difficulties which made the produced devices unusable. To overcome these difficulties, a miniaturization alternative, at the centimeter scale, using commercial MEMS microphones, has been carried out. Three cells have been built by different methods and have been tested for methane detection. The last cell generation can detect around 100 ppb of methane with a commercial interband cascade laser at 3.357 µm of wavelength and with 2.4 mW of optical power and an integration time of 1 second. Finally, to anticipate the next cell generation fabrication, a geometry optimization has been performed by simulation. This optimization shows that a 43 % signal improvement, compared to the most performant cell already built.

Pierre TCHOULFIAN

PhD degree (Institut National Polytechnique of Grenoble, France)

ELECTRICAL, OPTICAL, AND ELECTRO-OPTICAL PROPERTIES OF GAN MICROWIRES FOR THE FABRICATION OF LEDS.

This thesis deals with the characterization of GaN microwires (µwires) at the single wire level, toward the development of a light-emitting diode (LED) technology based on an ensemble of standing GaN µwires grown by metal organic vapour phase epitaxy. Each µwire is actually an LED consisting of an n-type core and a p-type shell, between which an InGaN/GaN multi quantum well active region is inserted. First, the electrical properties of the different parts of the n-type core were determined using resistivity measurements at the single wire level. The GaN:Si µwire exhibits conductivity values never reported by the planar layer counterparts. An original technique combining resistivity and thermoelectric measurements was developed to infer the electron density and mobility in these µwires. Spatially resolved optical measurements such as cathodoluminescence (CL) and µRaman confirmed the electron density values. The second part describes a spatially resolved study of the core-shell p-n junction using electron beam probing techniques. On a cleaved wire, the tridimensional (axial and radial) junction was highlighted by mapping the electric field (electron beam induced current, EBIC) or the electrostatic potential (secondary electron voltage contrast). These techniques yielded the donor and acceptor doping levels as well as the minority carriers diffusion lengths in the vicinity of the junction. EBIC mapping also provided the activation state of Mg dopants in the p-GaN:Mg shell. Finally, a study of the electro-optical properties of a single µwire LED, combined with EBIC and CL measurements, paves the way to the fabrication of more efficient µwire-based LED.

ANNUAL
RESEARCH REPORT
2015

OPTICS AND PHOTONICS

Contacts

Ludovic Poupinet
Head of the Optics and Photonics division
ludovic.poupinet@cea.fr

Laurent Fulbert
Deputy head of the Optics and Photonics division
Strategy and Programs Management
laurent.fulbert@cea.fr

Ivan-Christophe Robin
Marketing and Strategy Manager: Lighting & Photonic Devices
ivan-christophe.robin@cea.fr

François Simoëns
Marketing and Strategy Manager - Imaging Sensors
francois.simoens@cea.fr

Alexei Tchelnokov
Chief scientist
alexei.tchelnokov@cea.fr

Leti, technology research institute
Commissariat à l'énergie atomique et aux énergies alternatives
Minatec Campus | 17 rue des Martyrs | 38054 Grenoble Cedex 9 | France